Title
Biochemical Dissection of Microtubule-associated Protein Complex, MAP1B

Author
Tan, Tracy

Publication Date
2023

Peer reviewed|Thesis/dissertation

Biochemical Dissection of Microtubule-associated Protein Complex, MAP1B

By

TRACY TAN
DISSERTATION

Submitted in partial satisfaction of the requirements for the degree of

DOCTOR OF PHILOSOPHY

In

Biochemistry, Molecular, Cellular, and Developmental Biology

In the

OFFICE OF GRADUATE STUDIES

of the

UNIVIERISTY OF CALIFORNIA
DAVIS

Approved:

_____
Kassandra Ori-McKenney, Chair

_____
Daniel Starr

_____
Nitzan Shabek

Committee in Charge
2023

This is dedicated to my dear parents, Jinfa Tan(譚金發) and Tonghua Zhang(張彤華). Thank you for always believing in me, supporting me, and encouraging me to pursue my dreams.

Acknowledgment

I would first like to express my heartfelt gratitude to my thesis professor, Dr. Kassandra Ori-McKenney for her invaluable guidance, mentorship, and unwavering support. She believed in me and encouraged me, especially when I generated a lot of negative results from my experiments and was uncertain how to proceed with my thesis project. Her expertise, constructive feedback, and dedication have been instrumental in shaping the direction of my research. I also would like to thank Dr. Richard McKenney for his expertise in biochemistry and TIRF microscopy. I am truly grateful that he trained me from scratch when I first joined the MOM LAB! He has provided me with valuable advice on protein purification techniques and TIRF microscopy. In addition, I would like to thank all members in the MOM Lab for always sharing their knowledge and discussing experiment approaches together.

Next, I would like to thank my dissertation committee members, Dr. Dan Starr and Dr. Nitzan Shabek for valuable discussion and advice on my qualifying exam and dissertation meeting.

Finally, I am indebted to my family and friends for their unwavering encouragement and understanding. They belief in me has been a driving force, and I am immensely grateful for their unwavering support.

Abstract

Microtubules and actin are two essential cytoskeletal networks in neurons, providing structural support and serving as tracks for intracellular transport during neuronal morphogenesis and maintenance. The crosstalk between actin filaments and microtubules is important for various cellular processes such cell division, migration, vesicle and organelle transport, and axonal outgrowth. Microtubules provide platforms for many non-enzymatic microtubule-associated proteins (MAPs) and enzymatic motor proteins, which are responsible for intracellular transport. One non-enzymatic MAP, MAP1B, has been shown to have important functions in neural development due to its early expression in neurons. Previous studies have shown that knockdown of MAP1B results in defects in axon elongation and dendrite formation in neurons. Mutations in MAP1B are also associated with epilepsy. However, the molecular mechanism of how MAP1B regulates microtubule-based activities is still unclear.

To understand the basic function of MAP1B, we investigated its role in regulating actin- and microtubule-based activities. Our data revealed that both the Heavy Chain (HC) and Light Chain (LC) of MAP1B strongly bind to microtubules, but LC displayed a more diffuse behavior due to interactions with C-terminal tubulin tails. Both HC and LC also shield microtubules from severing by Spastin, although HC's protection was relatively weaker, possibly because it remains statically bound to microtubules rather than competing with Spastin for C-terminal tail of tubulins. MAP1B was also found to be a general inhibitor of various motor proteins, including kinesin-3, kinesin-4, and cytoplasmic dynein, by preventing access by these motors to the microtubule lattice.

The effect of MAP1B on actin was also explored. While both MAP1B LC and non-phosphorylated HC interact with actin filaments, HC's formation of an HC-LC complex hinders the binding of LC to actin filaments, thereby negatively regulating this interaction. Additionally, the phosphorylation of MAP1B HC 1-1500 by DYRK1A was shown to decrease its affinity for actin significantly, without a substantial impact on microtubule binding. In contrast, MAP1B LC's actin binding ability remained unaffected despite post-translational modifications.

Furthermore, MAP1B LC was found to bind actin monomers and directly facilitate actin polymerization over microtubules, creating a link between the two cytoskeletons. This action also enabled unanchored polymerized actin filaments to attach to adjacent microtubules, thereby connecting the two cytoskeletal networks, even without LC being statically bound to actin filaments. In addition, we have identified DYRK1A as key kinase that negatively regulates MAP1B HC's affinity for actin filaments.

In summary, this comprehensive study delves into the molecular mechanisms underlying MAP1B's involvement in mediating the interaction between actin and microtubules. It sheds light on the effects of both MAP1B HC and LC and their regulation by post-translational modifications, providing insights into its role during neuronal development and the pathology of associated neurological disorders.

Table of Contents

Chapter 1: Introduction

Cytoskeleton and Functions

The cytoskeleton is a major component of a living cell. It provides the structure and maintains the shape of a cell. The complex and dynamic cytoskeleton is involved in various cellular process, including cell division, cell signaling, transportation, and organization within the cell. There are three major types of filaments in a cell: actin-based microfilaments, tubulin-based microtubules, and intermediate filaments. The cytoskeleton components can rapidly assemble, dissemble, and reorganize in response to environmental cues and the needs of the cell. Actin and microtubules are essential during cell mitosis, neurite outgrowth and intracellular transport.

In the presence of ATP, G-actin monomers are polymerized into double stranded filaments called F-actin. Actin filaments are flexible and very dynamic. ATP-actin monomers are constantly added to the barbed end (plus-end) of the filament and depolymerizing from the pointed (minus-end) (Figure A). The resulting treadmilling of F-actin can be regulated by profilin

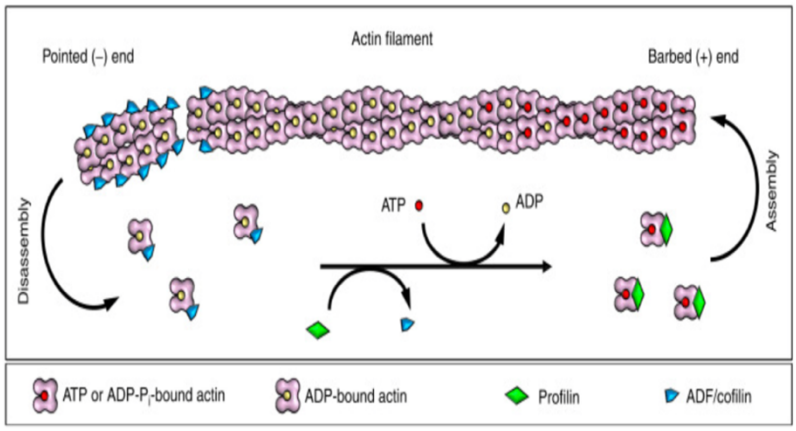

Figure A

The Comprehensive Sourcebook of Bacterial Protein Toxins (Fourth Edition), 2015

and cofilin by binding to

G-actin to catalyze exchange of ADP for ATP or binding to actin ADP within the filament to induce filament disassembly, respectively. Actin filaments have many crucial functions in cells. They can interact with cell membranes to provide strength and maintain the shape and structure of the cell. Actin filaments are enriched at the edges of cells to enable cell migration and crawling. They can also interact with myosin motors to enable the transport of organelles, vesicles, and other cellular materials to their appropriate locations within the cell. In neurons, they are enriched in the tips of axons and dendrites to facilitate growth cone elongation and guidance, and within dendritic spines, helping to initiate and stabilize synaptic connections. They also guide the migration of neurons to their appropriate destination within the brain during brain and nervous system development (reviewed in Coles & Bradke, 2015). Efficient synaptic communication and release of neurotransmitters is very important for neuronal activity. Actin filaments are involved not only in the establishment of dendritic spines, but in the guidance of synaptic vesicles into and within the presynaptic terminal.

Compared to actin, microtubules are larger, thicker and stiffer. Microtubules are long hollow tubes composed of $\alpha\beta$-tubulin heterodimers. The tubulin dimers are polymerized into linear protofilaments in a GTP-dependent process, resulting in predominantly 13-protofilament microtubules. The rigid and hollow rod-shaped microtubule is approximately 25 nm in diameter. The sequential addition of $\alpha\beta$-tubulins that align in head-to-tail manner give rise to microtubule polarity (Figure B). The α-tubulins are always exposed at the minus-end, while the β-tubulins are exposed at the plus-end. The growth rate of microtubules at the plus tip is faster than at the minus end due to this structural polarity. The third type of tubulin is called γ-tubulin and is often localized to centrosomes, but can be found in other foci of nucleation throughout the cell. It is a

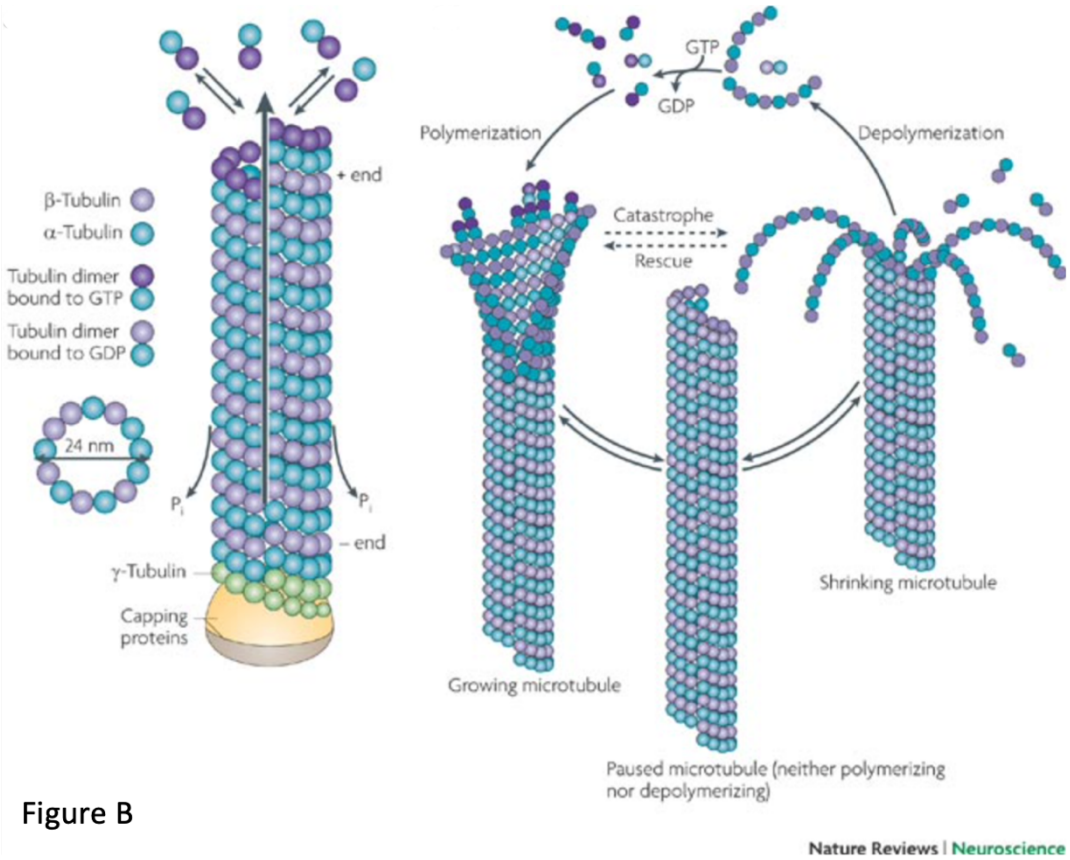

Figure B

critical factor for microtubule nucleation and anchoring (Kollman et al., 2011). Microtubules are highly dynamic and alternate between periods of growing and shrinking, which is termed dynamic instability. As the GTP-bound β-tubulin is incorporated into the microtubule lattice (often at the plus end), GTP is hydrolyzed to GDP, which decreasing its affinity to the adjacent molecule, resulting in destabilization and depolymerization of the microtubule known as catastrophe (Figure B). Microtubule dynamic instability that is defined as these periods of rapid growth and catastrophe is essential for many cellular functions. It contributes to the overall organization and reorganization of the cytoskeleton (Mitchison & Kirschner, 1984). Microtubule dynamic instability also plays an important role in the migration of chromosomes to the opposite side of the cell during mitosis and meiosis. Due to its importance in cell division, it has become the target of anti-cancer drugs. Several successful drugs that are used in chemotherapy for cancer

treatment target microtubules to regulate microtubule growth rate and stability (Jordan & Wilson, 2004). In migrating cells, microtubules can extend and retract, allowing the cell to change shape and move in response to environmental cues. Microtubules also serve as tracks for motor proteins, such as dynein and kinesins, in intracellular transport (Chevalier-Larsen & Holzbaur, 2006; Verhey & Hammond, 2009), which is essential to the overall health of a cell. Therefore, microtubules and microtubule-based activities must be tightly regulated.

Motor Proteins and Microtubule-associated Proteins (MAPs)

Neurons are highly polarized with distinct compartments, each serving different functions in transmitting electrical signals and processing information. Microtubules are essential for both the development and maintenance of these comparments and overall neuronal morphology, which enables neurons to connect and communicate with one another within a circuitry (Kapitein & Hoogenraad, 2015; Ramkumar et al., 2018). These cellular processes depend on proper regulation of microtubules, actin, and intracellular transport.

Microtubules provide platforms for many non-enzymatic microtubule-associated proteins (MAPs) and enzymatic motor proteins, which are responsible for intracellular transport. There are two major classes of motor proteins that move on the microtubule to transport a variety of cargo to different destinations precisely in the cytoplasm. Cytoplasmic dynein transports cargo to the minus ends of microtubules, while most transport kinesins carry cargo to the plus ends of microtubules(Chevalier-Larsen & Holzbaur, 2006). Mutations in motor proteins disrupt the intracellular transport balance and are associated with many neurodevelopmental and neurodegenerative diseases, such as Congenital fibrosis of the extraocular muscles (CFEOM),

which is a disorder that limits ocular motility (Cheng et al., 2014; Verhey & Hammond, 2009). Microtubule-associated proteins (MAPs) also bind on the microtubule lattice to regulate the dynamics of microtubules, as well as the binding and motility of motor proteins (Monroy et al., 2018, 2020). Previous studies and recent work from our lab have shown that some MAPs facilitate a specific type of motor while inhibiting others. MAPs can differentially regulate behaviors of other MAPs and motor proteins on the microtubule lattice(Lipka et al., 2016; Monroy et al., 2018, 2020). Some MAPs are able to bind on the microtubule simultaneously, whereas some exclude each other. The ability of some of these MAPs to stake out territory on the lattice therefore determines whether other MAPs, including motor proteins, can bind the microtubule. These "structural" MAPs can directly interact with certain motor proteins to promote their binding and motility on the microtubule lattice. However, MAPs can also block other motor proteins from accessing the microtubule and impede their transport functions. It is therefore very important to understand how MAPs regulate microtubule organization and microtubule-based transport.

Tau is one of the most well-studied MAPs because it is a hallmark of neurodegenerative disease, including Alzheimer's disease and some forms of frontotemporal dementia(Wang & Mandelkow, 2016). It has also been identified as a marker for brain damage after traumatic brain injury (TBI), highlighting its role in neurodegeneration. Although initially recognized for enhancing microtubule stability, tau has additional functions, such as controlling microtubule modifications, influencing microtubule mechanical properties, regulating microtubule motor transport, and more. Tau is mainly expressed in neurons during early brain development and continues throughout adulthood. There are six isoforms of tau found in brains. They are different

due to alternative splicing of Exon 2, 3 and 10, and contain either 3 or 4 microtubule-binding repeats. All six isoforms contain a 3 or 4 microtubule-binding repeats domain and are flanked by a proline-rich region and pseudo-repeats region. Tau was originally identified as a MAP that stabilizes and bundles microtubules. However, many studies have shown that tau also has other roles, such as directing motor transport and regulating microtubule lattice spacing. A recent study has shown that tau strongly inhibits kinesin-1 and kinesin-3, but has less effect on cytoplasmic dynein (Tan et al., 2019). It also contributes to stabilizing microtubules by forming "condensates" on the microtubules lattices and protecting it from severing by microtubule-severing protein, Spastin and katanin, which are expressed in all compartments within neurons to sever and generate short microtubules (Qiang et al., 2006; Tan et al., 2019). Tau is differentially phosphorylated in the adult brain and is mainly localized to axons. Many studies have shown that hyperphosphorylation of tau reduces its affinity for microtubules and promote formation of aggregates. Tau aggregates have a high tendency to form paired helical filaments (PHFs) and are suggested to be associated with neurogenerative diseases such as Alzheimer's disease. Many mutations in tau and hyperphosphorylation at serine-proline or threonine-proline motifs are suggested to have a higher tendency to form aggregates and lead to tauopathies (reviewed in Wang & Mandelkow, 2016). Although phosphorylation of tau decreases its affinity for microtubules, it does not always lead to the formation of aggregates into PHFs. An early study shows that phosphorylation of tau at KXGS motifs such as S324 and S214 causes tau to detach from microtubule, but inhibits it from forming PHFs (Schneider et al., 1999). While most studies focus on phosphorylation sites causing tau to dissociate from microtubules and form aggregates, site-specific phosphorylation of tau at Serine 262 affects its interaction with End-binding protein-

1 (EB1) without causing dissociation from microtubules. Therefore, phosphorylation of tau at different sites regulates other functions of this protein and potentially contributes to the organization of the cytoskeleton.

MAP1B is highly expressed during early stages of neuronal development and is downregulated in the adult brain (Garner et al., 1990; Tucker et al., 1988). It is localized in neuronal somas, dendrites, and distal parts of axons (reviewed in Villarroel-Campos & Gonzalez-Billault, 2014). MAP1B is encoded as a polypeptide chain and first synthesized to a polyprotein, and then proteolytically cleaved into a heavy chain (HC) and light chain (LC), which can associate to form a protein complex (Halpain & Dehmelt, 2006; Hammarback et al., 1991; Villarroel-Campos & Gonzalez-Billault, 2014). Both MAP1B HC and LC contain microtubule and actin binding domains (Noble et al., 1989; Tögel et al., 1998). The two microtubule binding domains of MAP1B reside at amino acids 589-787 in HC and 2203-2239 in LC (Noble et al., 1989; Tögel et al., 1998). A prior study also suggested a putative third microtubule binding domain between the first 126 amino acids of HC that can bind soluble tubulins *in vitro* (Gomi & Uchida, 2012). MAP1B also promotes microtubule assembly (Kuznetsov et al., 1981).

MAP1B is a major component of the neuronal cytoskeleton (Bloom, Luca, & Vallee, 1985). Mutations in MAP1B have been shown to be associated with many neurological diseases(Cheng et al., 2014; Heinzen et al., 2018). An early study showed that MAP1B is necessary for proper dendritic spine formation (Tortosa et al., 2011). They observed a significant decrease of mature dendritic spines in neurons and an increased number of aberrant filipodia-like protrusions in the absence of MAP1B. Defects in axonal elongation and branching, and neuronal migration were also observed in MAP1B gene-disrupted mice (Bouquet et al., 2004; Takei et al., 2000). A recent

study identified de novo and inherited variants in MAP1B in periventricular nodular heterotopia (PVNH), which is a disorder that leads to abnormal migration of neurons during fetal brain development (Heinzen et al., 2018). The identified variants in PVNH include one de novo mutation that leads to a premature stop codon and the expression of a truncated MAP1B (aa 1-303) and two inherited alleles that lead to premature stop codons and the expression of a truncated MAP1B (aa 1-532 and aa 1-1103). Another recent study showed that MAP1B interacts with a kinesin-4, KIF21A. The gain-of-function mutations in KIF21A cause defects in axon elongation and enlargement of growth cone in the oculomotor nerve (Cheng et al., 2014). KIF21A is normally in an autoinhibited state, like many other kinesin motors (Chiba et al., 2019; Verhey & Hammond, 2009). The mutations in the KIF21A protein are gain-of function, because they release this autoinhibition. This overactivity of the motor is hypothesized to lead to CFEOM (Bianchi et al., 2016; Cheng et al., 2014; van der Vaart et al., 2013). Intriguingly, MAP1B knockout mice also develop CFEOM, whose phenotypes mimic the phenotypes of the KIF21A mutant mice (Cheng et al., 2014).

Actin-Microtubule Crosstalk

Microtubules and actin are two essential components of the cytoskeleton in neurons, providing structural support and facilitating intracellular transport. The crosstalk between microtubules and actin plays a crucial role in various neuronal processes, including cell morphology, axon guidance, synaptic plasticity, and vesicle trafficking (Mohan & John, 2015). The interaction between microtubules and actin helps maintain the unique morphology of neurons (reviewed in Dehmelt and Halpain, 2004). Microtubules provide the structural framework,

guiding the elongation of axons and dendrites, while actin filaments contribute to the growth and stability of dendritic spines and axonal growth cones (Mohan & John, 2015). During neuronal development, axons navigate through complex environments to reach their target destinations. The coordination between microtubules and actin is crucial for proper axon guidance (Mohan & John, 2015). Microtubules guide the overall direction of axonal growth, while actin dynamics at the growth cone's leading edge play a role in responding to guidance cues (Dent & Gertler, 2003). Actin filaments are involved in the dynamic changes of dendritic spines, which are crucial for synaptic plasticity (Tortosa et al., 2011), the basis for learning and memory. Intracellular transport of vesicles and organelles in neurons depends on both microtubules and actin filaments. Microtubules act as "highways" for long-range transport, while actin provides the "local streets" for fine-tuned and shorter-distance transport within dendrites and axons (Evans et al., 2014). Both microtubules and actin are involved in the trafficking of membrane vesicles during endocytosis and exocytosis at the synapse (Zhu et al., 2009). The coordinated action of these cytoskeletal components ensures efficient communication between neurons. In developing brains, neurons need to migrate to their appropriate positions. In migrating neurons, microtubules extend into the leading process, stabilizing it, while actin-rich structures like lamellipodia and filopodia drive the movement by pushing the process forward (Dehmelt & Halpain, 2004). Overall, the intricate crosstalk between microtubules and actin is essential for the proper functioning of neurons. Disruptions in this crosstalk can lead to neuronal developmental disorders, neurodegenerative diseases, and impaired synaptic communication. Understanding the molecular mechanisms underlying microtubule-actin interactions in neurons is a topic of ongoing research in neuroscience.

Structural MAPs, such as MAP1B and tau were originally identified and categorized as microtubule-binding and stabilizing proteins since they co-purified with polymerized brain tubulin (Bloom, Luca, & Vallee, 1985). However, many studies have shown that they contribute to a variety of other molecular roles, such as directing motor transport and crosslinking actin filaments and microtubules. Both MAP1B and tau have been reported to bind to both microtubules and actin filaments. However, MAP1B does not share any sequence similarity to tau (Tucker, 1990). Nevertheless, they are the MAPs capable of binding both actin and microtubules, a feature that is not present in the majority of other MAPs. They have been identified as the key players that directly crosslink the two cytoskeletons (reviewed in Mohan and John, 2015). Therefore, it is important to understand the molecular mechanism of how MAPs regulate these two cytoskeletal networks and contribute to overall neuronal health.

Chapter 2: Biochemical Dissection of Microtubule-associated Protein Complex, MAP1B

Introduction

MAP1B is a neuron-specific microtubule associated protein (MAP), which is predominantly expressed in axons during early neuronal development and subsequently downregulated. However, it is also expressed in the dendrites, pre- and post-synaptic densities, and dendritic spines of mature neurons in areas showing significant synaptic plasticity in adult brains (Bodaleo et al., 2016; Mohan & John, 2015; Tortosa et al., 2011). MAP1B is required for dendritic spine formation through regulation of actin (Tortosa et al., 2011). MAP1B was regulated by phosphorylation. Certain proline-directed proteins kinases, such as GSK3β and DYRK1A, phosphorylate MAP1B, and this specific phosphorylation type is referred to as mode-I phosphorylation. It has been reported that mode-I phosphorylation of MAP1B was found enriched in distal ends of growing axons (Villarroel-Campos & Gonzalez-Billault, 2014), and most functions of MAP1B are regulated by this type of phosphorylation, which is reported to affect actin dynamics and cytoskeletal crosslinking (Del Río et al., 2004). In addition, mode-I phosphorylation of MAP1B was found to be a downstream effector of the Netrin 1-signaling pathway that is critical in neuronal migration and axonal guidance (Del Río et al., 2004). Another recent study also showed that MAP1B-deficient mice mimic the phenotype of kinesin-4 gain-of-function mutant mice, which lead to aberrant development of axons and growth cones in oculomotor nerves, resulting in the development of congenital fibrosis of extraocular muscles type 1 (CFEOM1) (Cheng et al., 2014).

Although the phenotypic effects of MAP1B in neural development have been extensively studied *in vivo,* the underlying molecular mechanisms of MAP1B on microtubules and actin filaments are still unclear. Here, we present a comprehensive analysis of the binding behaviors of MAP1B, both HC and LC, on actin filaments and microtubules. Our findings revealed that the MAP1B LC displayed a more diffusive binding behavior than MAP1B HC on the microtubule lattice and protected the lattice from severing by Spastin through interactions with the C-terminal tails of tubulins. MAP1B appears to be a general inhibitor of many motor proteins, because both HC and LC impede motors from accessing microtubule lattice, including kinesin-3, kinesin-4 and cytoplasmic dynein. In contrast, they have different functions in regulating cytoskeletal organization. We found that MAP1B phosphorylation of HC by DYRK1A negatively regulates its affinity to actin filament. Interestingly, MAP1B HC negatively regulates MAP1B LC's affinity to actin by masking its actin binding domain. Moreover, our data suggested that MAP1B LC is able to direct actin polymerization along microtubules and crosslink these two cytoskeletons without being statically bound to actin filaments. Overall, we have identified a MAP that is capable of binding to both the microtubule and actin cytoskeletal networks and determined how this activity is regulated by phosphorylation, providing insight into its role in neurons.

Results

MAP1B heavy chain (HC) and light chain (LC) have high affinity to microtubules

MAP1B is first synthesized as a polyprotein and proteolytically cleaved to form a heavy chain (HC: aa 1-2202) and a light chain (LC: aa 2203-2464). Figures 1A shows a schematic representation of mouse MAP1B. Both HC and LC contain actin binding domains and microtubule

binding domains. The LC has been reported to interact with the N-terminus of the HC. Using Alphafold, we predicted the structures of MAP1B HC 1-1500 and LC. There are two globular domains in the HC: aa 27-240 and aa 241-532. The rest of HC is intrinsically disordered. There is one globular domain at the C-terminus of LC at aa 2340-2464, which is also reported to be the actin binding domain (figure 1C). There are more than 33 phosphorylation sites within the HC, but not many known kinases (Scales et al., 2009). Previous studies have found that GSK3β phosphorylates MAP1B HC at S1260, T1265, S1390, and DYRK1A phosphorylates MAP1B HC at S1395. Many studies have shown that phosphorylation of MAP1B HC regulates its affinity to microtubules and actin *in vivo* (reviewed in Riederer, 2007), we will investigate the effects of MAP1B phosphorylation on the cytoskeleton in vitro later in this study.

To understand the binding behaviors of MAP1B on microtubules, we first characterized the regions of MAP1B that robustly bind to microtubules. For these experiments, we used purified recombinant proteins in in vitro reconstitution assays. We cloned a variety of MAP1B HC and LC constructs with fluorescent tags, expressed the constructs in bacterial or insect cells, and purified them using different types of column chromatography. We directly imaged the binding of MAP1B to taxol-stabilized microtubules *in vitro* using TIRF microscopy. A recent study has identified new loss-of-function heterozygous variants in MAP1B, including de novo and parental inheritable variants that are associated with PVNH (Heinzen et al., 2018). All three of these variants result in premature stop codons. Hence, we first examined whether the three epilepsy-associated mutant variants of MAP1B could bind microtubules. We added fluorescently labeled MAP1B 1-303, 1-532 and 1-1103 to flow chambers with taxol-stabilized microtubules affixed to coverslips, and imaged their molecular behaviors using TIRF microscopy. The epilepsy-associated mutant,

MAP1B 1-303, which only contains one putative microtubule binding domain, does not bind to microtubules (figure 1B). The second mutant, MAP1B 1-532 weakly binds to microtubes (figure 1B) with a Kd=74.38 (Supplementary figure 1). Increasing concentrations up to 500 nM of both variants were tested, but they still did not saturate the microtubule (Supplementary figure 1).

Although previous studies have shown that MAP1B 1-126 interacts with tubulin (Gomi & Uchida, 2012), the interactions of MAP1B 1-303 and 532 with microtubules were weak. However, the longest epilepsy-associate mutant, MAP1B 1-1103 exhibited a high affinity for microtubules, with a Kd of 1.58 (Supplementary figure 1). At 5nM of MAP1B 1-1103, it shows robust binding to the microtubules (figure 1B). We also examined purified recombinant MAP1B HC MTBD (aa 639-747), MAP1B 1-1500, and full length HC and LC, and found that they all bound to taxol-stabilized microtubules with high affinity (figure 1B). Together, these data suggest that the MTBD 639-747 of MAP1B is necessary for robust microtubule binding.

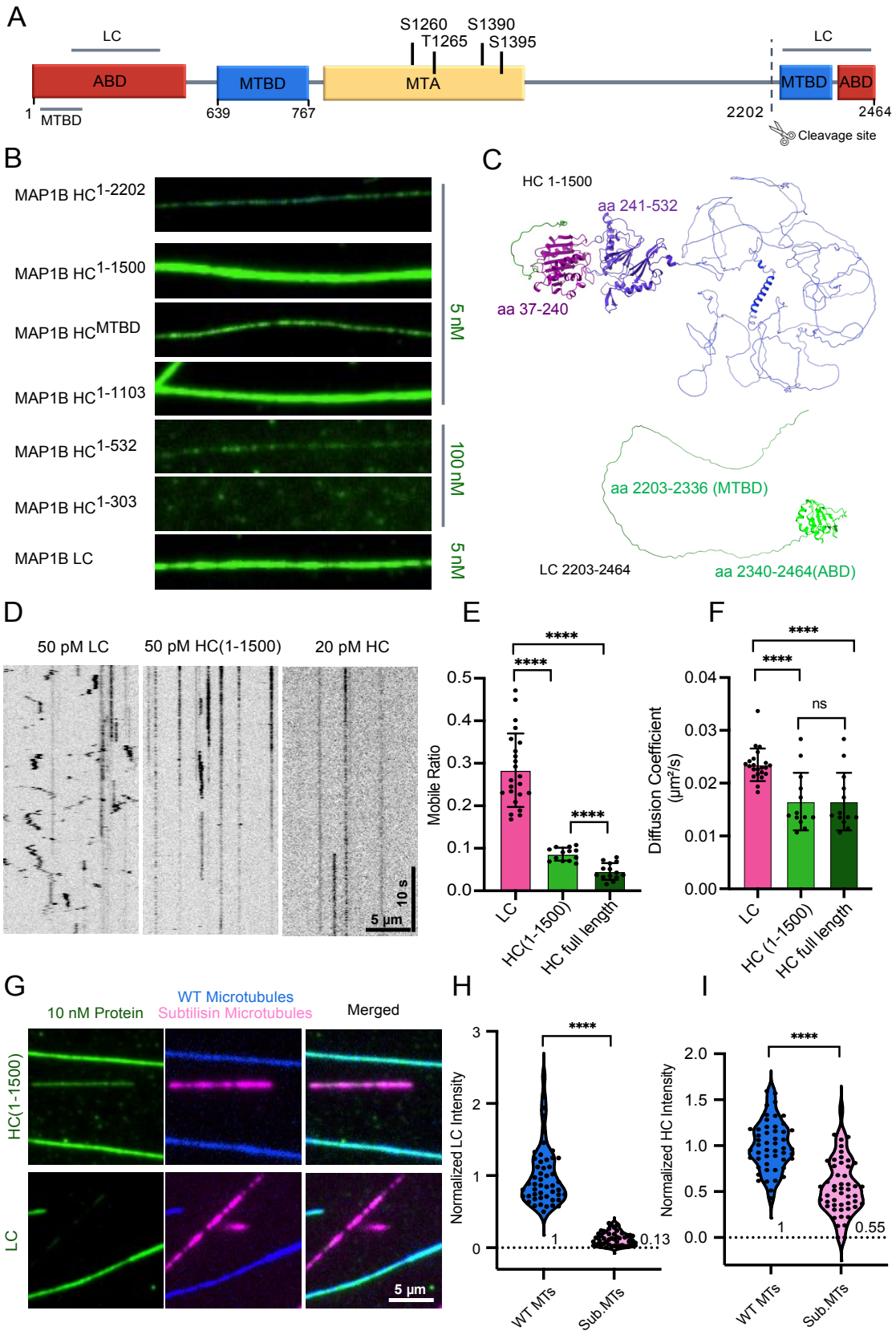
A
LC
ABD
MTBD
MTA
S1260
T1265
S1390
S1395
LC
MTBD
ABD
1
MTBD
639
767
2202
2464
Cleavage site
B
MAP1B HC1-2202
MAP1B HC1-1500
MAP1B HCMTBD
MAP1B HC1-1103
MAP1B HC1-532
MAP1B HC1-303
MAP1B LC
5 nM
100 nM
5 nM
C
HC 1-1500
aa 241-532
aa 37-240
aa 2203-2336 (MTBD)
LC 2203-2464
aa 2340-2464(ABD)
D
50 pM LC
50 pM HC(1-1500)
20 pM HC
10 s
5 µm
E
Mobile Ratio
LC
HC(1-1500)
HC full length
F
Diffusion Coefficient (µm²/s)
ns
LC
HC (1-1500)
HC full length
G
10 nM Protein
WT Microtubules
Subtilisin Microtubules
Merged
HC(1-1500)
LC
5 µm
H
Normalized LC Intensity
1
0.13
WT MTs
Sub.MTs
I
Normalized HC Intensity
1
0.55
WT MTs
Sub.MTs

Figure1. Analysis of MAP1B HC and LC microtubule binding behaviors. (A) Schematic representation of MAP1B. Red box is actin binding domain (ABD) in the HC (1-508). Blue box is microtubule binding domain (MTBD) in the HC (639-767). LC also contains ABD and MTBD. Yellow box is a putative microtubule assembly domain (MTA) in the HC (976-1401). A putative second MTBD in HC (1-126) was also reported. The cleavage site at aa2202 is conserved among many species including human, rat and drosophila. Phosphorylation sites by known kinases within the HC are presented. (B) TIRF-M images of purified fluorescently tagged MAP1B HC full length, MAP1B HC 1-1500, MAP1B HC microtubule binding domain, MAP1B HC 1-1103, MAP1B LC at 5 nM concentrations and MAP1B HC 1-532, MAP1B HC 1-303 at 100 nM concentrations on taxol-stabilized microtubules. (C) Alphafold predicted structures of MAP1B HC 1-1500 and LC. (D) Kymographs of MAP1B LC, HC 1-1500 and HC full length on taxol-stabilized microtubules from single molecule assays. (E-F) Quantification of the mobile ratios and diffusion coefficients of MAP1B LC, HC 1-1500 and HC full length on the microtubules. The total trajectories analyzed are n=13914, 645, 622 from 2 independent experiments. ****p<0.0001. (G) TIRF-M images of MAP1B HC 1-1500 and LC on mixed subtilisin-treated (magenta) and wild type microtubules (blue). (H) Quantification of MAP1B HC 1-1500 and LC on subtilisin-treated microtubules (n=50) and wild type microtubules (n=50) from 2 independent trials. ****p<0.0001. All graphs show all datapoints. P-values were determined using an unpaired student's t-test.

MAP1B light chain (LC) is more diffusive on microtubules than heavy chain (HC) due to its interaction with the tubulin C-terminal tails.

To examine the difference of MAP1B HC and LC binding behaviors on microtubules, we performed single molecule assays using TIRF microscopy. We added 50 pM of HC full length, HC 1-1500, or LC to flow chambers and image single molecular behaviors of MAP1B on microtubules. We observed that LC exhibits a diffusive binding behavior on the microtubule while most of HC full length and HC 1-1500 remain statically bound (figure 1D). To measure the difference in this binding behavior, we analyzed the mobile ratio of HC and LC molecules on the microtubules. We observed that 28% of LC molecules on the microtubule are mobile, while only 8% of HC 1-1500 and 4% of HC full length molecules are mobile (figure 1E). We also measured the diffusion rate of LC, HC 1-1500 and HC full length and compared the diffusion coefficients. The diffusion rate of LC was also higher than HC 1-1500 and HC full length (figure 1F). However, the diffusion rate of MAP1B HC 1-1500 and HC full length were not significantly different. These data indicate that LC displays a more diffusive behavior than HC on the microtubule lattice. We next wanted to determine the reason for the difference in the HC and LC diffusive behaviors. We used subtilisin-digested microtubules to examine the effect of the C-terminal tails of tubulin on MAP1B. Subtilisin treatment of microtubules digests the C-terminal tails of tubulin. We mixed wild-type microtubules and subtilisin-treated microtubules in different fluorescent dye and immobilized them in the flow chamber. We then added either 10 nM of MAP1B HC 1-1500 or LC to the mixed microtubule populations and observed their binding behaviors. Our data indicate that both MAP1B HC 1-1500 and LC have lower affinity to microtubules that lack C-terminal tails. However, removal of C-terminal tails has a more pronounced effect on LC binding than HC 1-1500 (figure 1G). We normalized the fluorescent intensity of LC or HC 1-1500 on subtilisin-treated microtubules to wildtype microtubules. We observed that only 13% of LC (figure 1H) were bound

to subtilisin-treated microtubules, whereas 55% of HC 1-1500 molecules were bound to subtilisin-treated microtubules compared to the association of each construct with wild-type microtubules (figure 1I). These data indicate that LC utilizes the C-terminal tails of tubulin to bind and diffuse along the microtubule lattice. While HC 1-1500 interacts with the C-terminal tails of tubulins, these interactions may be less important for its more static association with microtubules. Therefore, MAP1B LC displays a more diffusive behavior on microtubule compared to MAP1B HC.

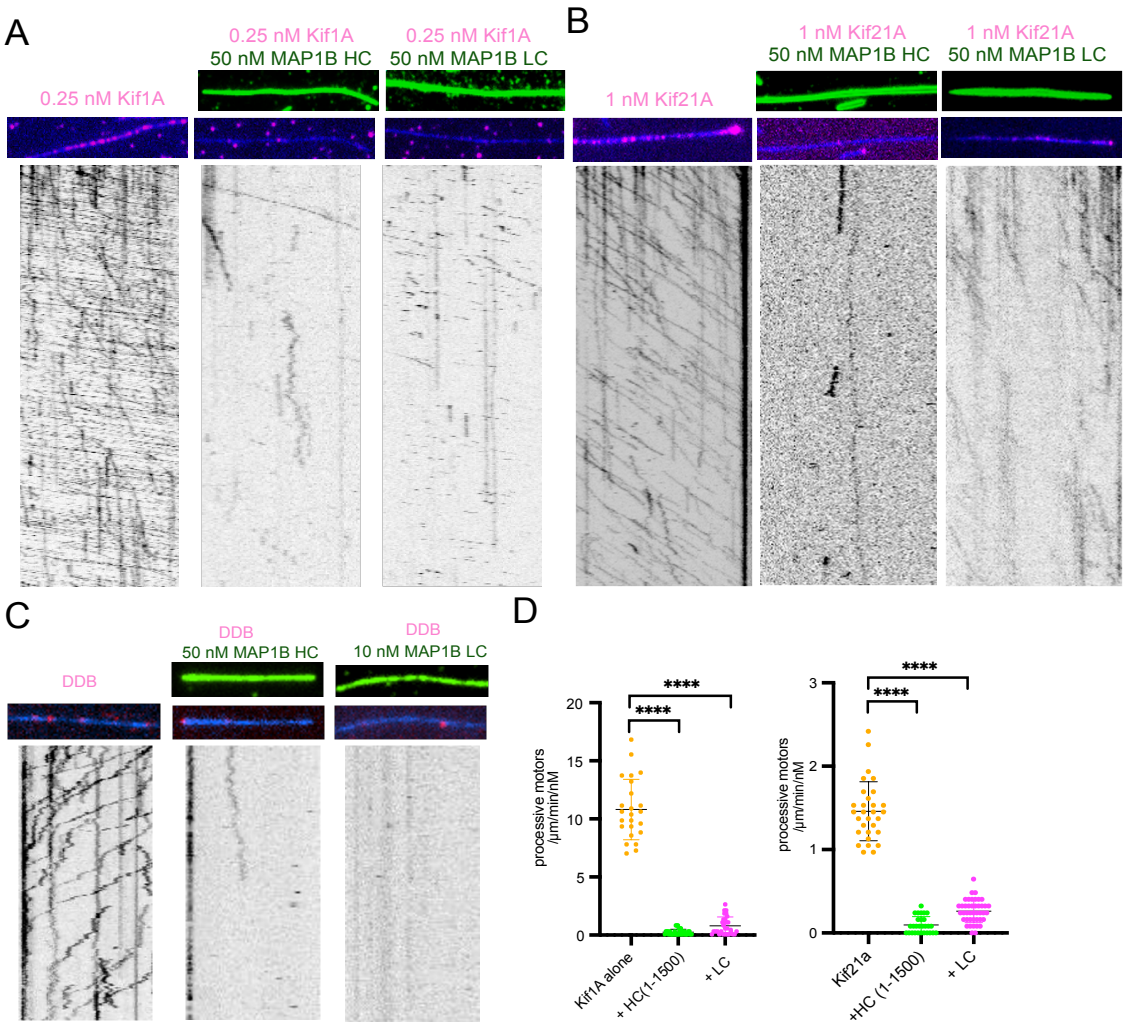
A
0.25 nM Kif1A
0.25 nM Kif1A
50 nM MAP1B HC
0.25 nM Kif1A
50 nM MAP1B LC
B
1 nM Kif21A
1 nM Kif21A
50 nM MAP1B HC
1 nM Kif21A
50 nM MAP1B LC
C
DDB
DDB
50 nM MAP1B HC
DDB
10 nM MAP1B LC
D
processive motors
/µm/min/nM
****
****
Kif1A alone
+ HC(1-1500)
+ LC
processive motors
/µm/min/nM
****
****
Kif21a
+HC (1-1500)
+ LC
E
100 nM Spastin Alone
25 nM MAP1B HC
100 nM Spastin
25 nM MAP1B LC
100 nM Spastin
0 min
10 min
0 min
10 min
0 min
10 min
MT
Spastin
HC
LC
F
Normalized Microtubule Intensity
****
****
0.11
0.51
0.81
0.71
Spastin alone
+ MAP1B HC
+ MAP1B LC
MTs alone

Figure 2. The effects of MAP1B HC 1-1500 and LC on motor proteins and spastin. (A)TIRF-M images and kymographs of 0.25 nM of KIF1A-mScarlet + 1 mM ATP in the absence and presence of 50 nM of sfGFP-MAP1B HC 1-1500 and LC-sfGFP. (B) TIRF-M images and kymographs of 1 nM of KIF21A (1-930) -mScarlet + 1 mM ATP in the absence and presence of 50 nM of sfGFP-MAP1B HC 1-1500 and LC-sfGFP. (C) TIRF-M images and kymographs of dynein-dynactin-BicD2(DDB)-TMR + 1 mM ATP in the absence and presence of 50 nM of sfGFP-MAP1B HC 1-1500 and 10 nM LC-sfGFP. (D) Quantifications of landing rates of processive KIF1A, KIF21A, and DDB in the absence and presence of MAP1B HC 1-1500 and LC. (E) TIRF-M images of purified, recombinant TMR-labeled SNAP-Spastin either alone or in the presence of either sfGFP-MAP1B HC 1-1500 or LC-sfGFP. (F) Quantification of microtubule intensity difference after severing by spastin of spastin alone (n=40 microtubules), in the presence of HC 1-1500 (n=29 microtubules) and LC (n=50) from 2 independent experiments, ****$p<0.0001$. All graphs show all datapoints. P-values were determined using an unpaired student's t-test.

MAP1B is a general inhibitor of motor proteins.

It has been reported that MAP1B is expressed in both axons and dendrites in neurons (reviewed in Villarroel-Campos & Gonzalez-Billault, 2014). MAPs can differentially regulate motility of different types of motor proteins on the microtubule lattice (Monroy et al., 2018, 2020). A recent study has identified that members of the kinesin-3 and kinesine-4 families are responsible for cargo transport into both dendrites and axons, while most other kinesins are either non-transport motors or selectively transport cargo into axons (Lipka et al., 2016). We wanted to examine how MAP1B affects the binding and motility of kinesin-3 (KIF1A) and

kinesin-4 (KIF21A) on the lattice. Our data revealed that both KIF1A and KIF21A were largely inhibited from landing on the microtubules by the presence of MAP1B HC 1-1500 and MAP1B LC (figure 2A-B). We then examined the effects of MAP1B on cytoplasmic dynein. Previous studies have shown that different MAPs selectively regulate different kinesins but have insignificant effects on cytoplasmic dynein (Monroy et al., 2018, 2020; Tan et al., 2019). Interestingly, we observed that MAP1B HC 1-1500 and LC also impeded the processive DDB complex from landing on microtubules (figure 2C). Our data has revealed that MAP1B act as a general inhibitor to many motors and restricts them from accessing the microtubule lattice.

MAP1B LC protects microtubules from severing by spastin.

Next, we wanted to examine how MAP1B affected other proteins on the microtubule lattice. Spastin is a microtubule severing enzyme. It is an ATPase that hydrolyzes ATP to sever microtubules and generate short microtubule seeds in cells(Roll-Mecak & McNally, 2010) . It "pulls" the C-terminus of tubulins to destabilize tubulin-tubulin interactions and destruct the microtubule lattice (Roll-Mecak & Vale, 2008). A previous study has shown that tau "condensates" that formed on microtubules protected the underlying microtubule lattice from severing by spastin (Tan et al., 2019). We found that both MAP1B HC 1-1500 and LC protects microtubules from severing by spastin (figure 2E). Our analysis from a time-course movie showed that the fluorescence intensity of microtubules after severing by spastin was reduced by 89% compared to fluorescence intensity of unsevered microtubule, indicating our spastin robustly severs undecorated microtubules. In the presence of MAP1B HC 1-1500, the fluorescence intensity of microtubules in the presence of spastin was reduced by 49%, while

the fluorescence intensity dropped by 19% in the presence of MAP1B LC (figure 2F). These data indicate that the LC more effectively protects the microtubule lattice from spastin severing compared to the HC.

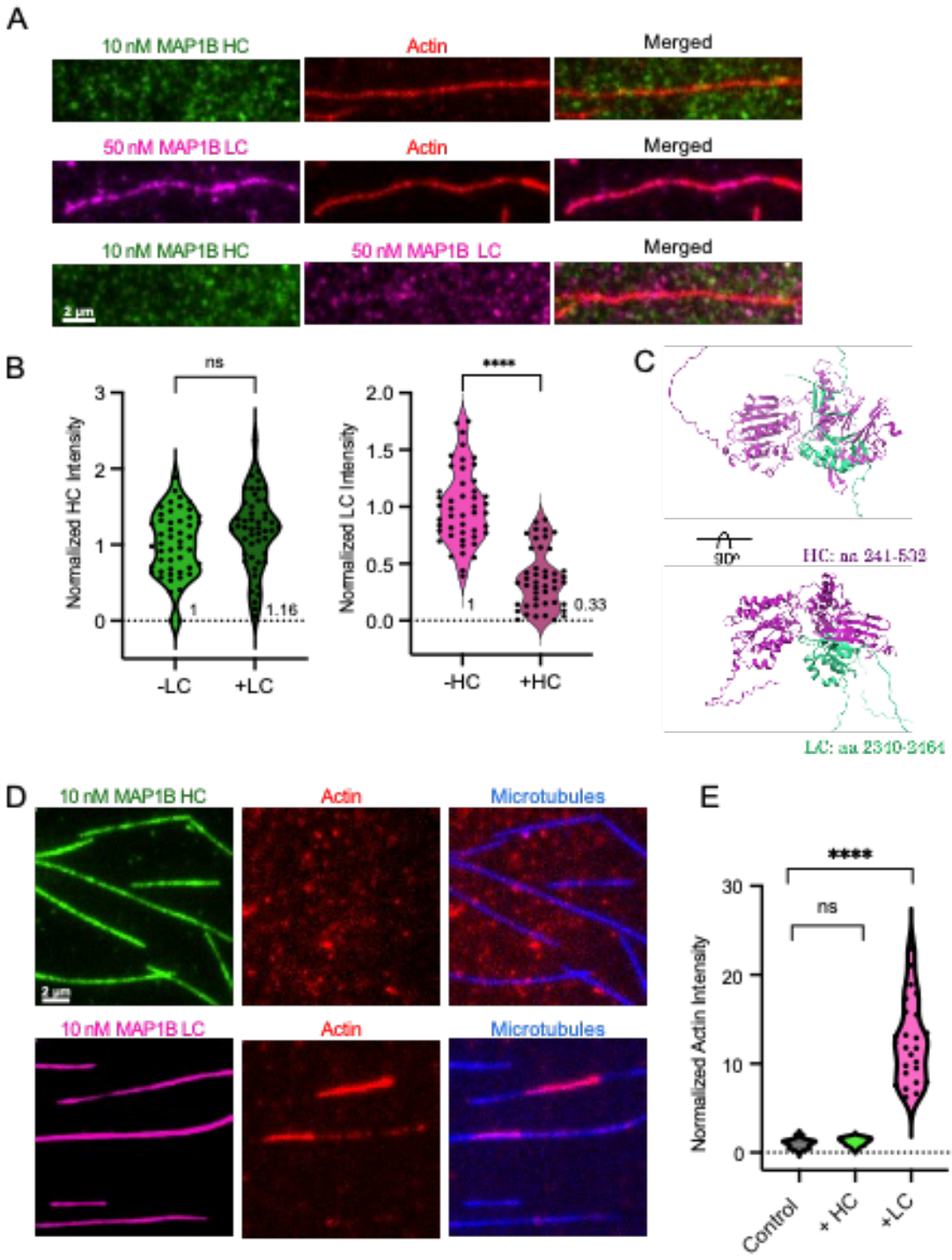

Figure 3. LC binds actin but HC does not. (A) TIRF-M images of MAP1B HC full length-sfGFP and LC-mScarlet on actin filaments. (B) Quantification of fluorescence intensity of MAP1B HC full length on actin filaments in the absence and presence of MAP1B LC (n=50 actin filaments from 2

independent trials, ****p<0.0001) and fluorescence intensity of MAP1B LC on actin filaments in the absence and presence of MAP1B HC full length (n=50 actin filaments from 2 independent trials, ****p<0.0001). (C) Alphafold prediction of HC-LC complex interaction region: HC 241-532 interacts with LC 2340-2464, which is the reported actin binding domain of LC. (D) TIRF-M images of either MAP1B HC full length or MAP1B LC and actin filaments on immobile microtubules. (E) Quantification of actin fluorescence intensity in the absence or presence of MAP1B HC full length or LC on microtubules. All graphs show all datapoints. P-values were determined using an unpaired student's t-test.

MAP1B HC negatively regulates LC's affinity to actin filaments.

Since MAP1B HC and LC have both actin and microtubule binding domains, we also wanted to examine the binding behaviors of MAP1B to actin. We added either MAP1B HC full length or MAP1B LC to the flow chamber with coverslips coated with immobile actin filaments and imaged their binding behaviors using TIRF-M. We observed that MAP1B LC binds to actin filaments, but MAP1B HC does not (figure 3A). We then mixed MAP1B HC full length and LC to examine how they affect each other. Surprisingly, we observed that the presence of MAP1B HC significantly decreased LC's affinity to actin filaments. MAP1 HC does not bind to actin filaments, regardless of the presence or absence of MAP1B LC (figure 3B). However, the fluorescence intensity of MAP1B LC on actin filaments decreased by 67% in the presence of MAP1B HC, indicating that MAP1B HC negatively affected MAP1B LC's binding to actin (figure 3B). It has been reported that COOH terminus of MAP1B LC interacts with actin, and this region

also associates with the N-terminus of the HC to form a HC-LC complex (Tögel et al., 1998). Using Alphafold, we predicted the HC-LC interaction region in MAP1B LC was aa 2340-2464, which is also the putative actin binding domain of LC. The data suggests that the presence of MAP1B HC interacts with COOH terminus of LC, preventing its association with actin filamentse by masking LC's actin binding domain (figure 3C).

MAP1B LC is able to recruit actin filaments to microtubules.

Our data has shown that LC can bind to both microtubules and actin filaments. Next, we wanted to examine whether MAP1B LC can recruit actin filaments to microtubules and crosslink these two cytoskeletons. We added MAP1B HC or LC and actin filaments to flow chamber with coated immobile microbubbles and imaged on TIRF-M. MAP1B LC showed robust binding to microtubules, and was able to recruit actin filaments to microtubules effectively (figure 3D). However, consistent with our earlier data, MAP1B HC binds to microtubules but was not able to recruit actin filaments to microtubules (figure 3D-E). Although both MAP1B HC and LC have been reported to have microtubule and actin binding domains (reviewed in Villarroel-Campos & Gonzalez-Billault, 2014), only MAP1B LC is capable of binding and crosslinking these two cytoskeletal networks.

Phosphorylation of MAP1B HC by DYRK1A negatively regulates actin binding affinity

An earlier study reported that only dephosphorylated MAP1B binds to microfilaments (Pedrotti & Islam, 1996). To investigate how phosphorylation of MAP1B HC affect its affinity to actin filaments, we compared the actin binding behaviors of non-phosphorylated and

phosphorylated MAP1B HC 1-1500. We observed that bacterially expressed MAP1B HC (1-1500) binds to actin filaments while insect cell-expressed MAP1B does not (figure 4A-4B). Bacterially expressed MAP1B HC(1-1500) does not have any post-translational modifications compared to the insect cell-expressed protein.

According to previous studies, DYRK1A is one of the kinases that phosphorylates MAP1B HC. We performed kinase assays with DYRK1A and bacterially expressed-MAP1B HC 1-1500 for 30 minutes *in vitro*. We then analyzed the western blots with phosphor-Ser/Thr antibody to validate the kinase assays. DYRK1A was able to phosphorylate MAP1B HC 1-1500 *in vitro* (figure 4C). We then mixed bacterially expressed MAP1B HC(1-1500) and DYRK1A with or without ATP, and for the phosphorylation assay to proceed for 30mins, then imaged the binding behaviors of either non-phosphorylated or phosphorylated MAP1B on actin filaments using TIRF-M. Strikingly, we observed that non-phosphorylated MAP1B HC 1-1500 binds actin, whereas the DYRK1A phosphorylated MAP1B HC 1-1500 does not (figure 4D).

Next, we wanted to investigate the effects of MAP1B HC phosphorylation on its microtubules binding behaviors. We allowed DYRK1A to phosphorylate MAP1B HC 1-1500 for 30 mins and imaged MAP1B HC on microtubules. We observed that the phosphorylated MAP1B HC 1-1500 has a slight decrease in fluorescence intensity on microtubules compared to the non-phosphorylated condition (figure 4F). Compared to the non-phosphorylated MAP1B HC 1-1500, the fluorescence intensity of HC on microtubules dropped by 21% (figure 4G). In contrast, upon phosphorylation by DYRK1A, MAP1B HC 1-1500's affinity to actin filaments dropped by 75% (figure 4E). Phosphorylation of MAP1B HC by DYRK1A therefore predominantly affects its affinity for actin.

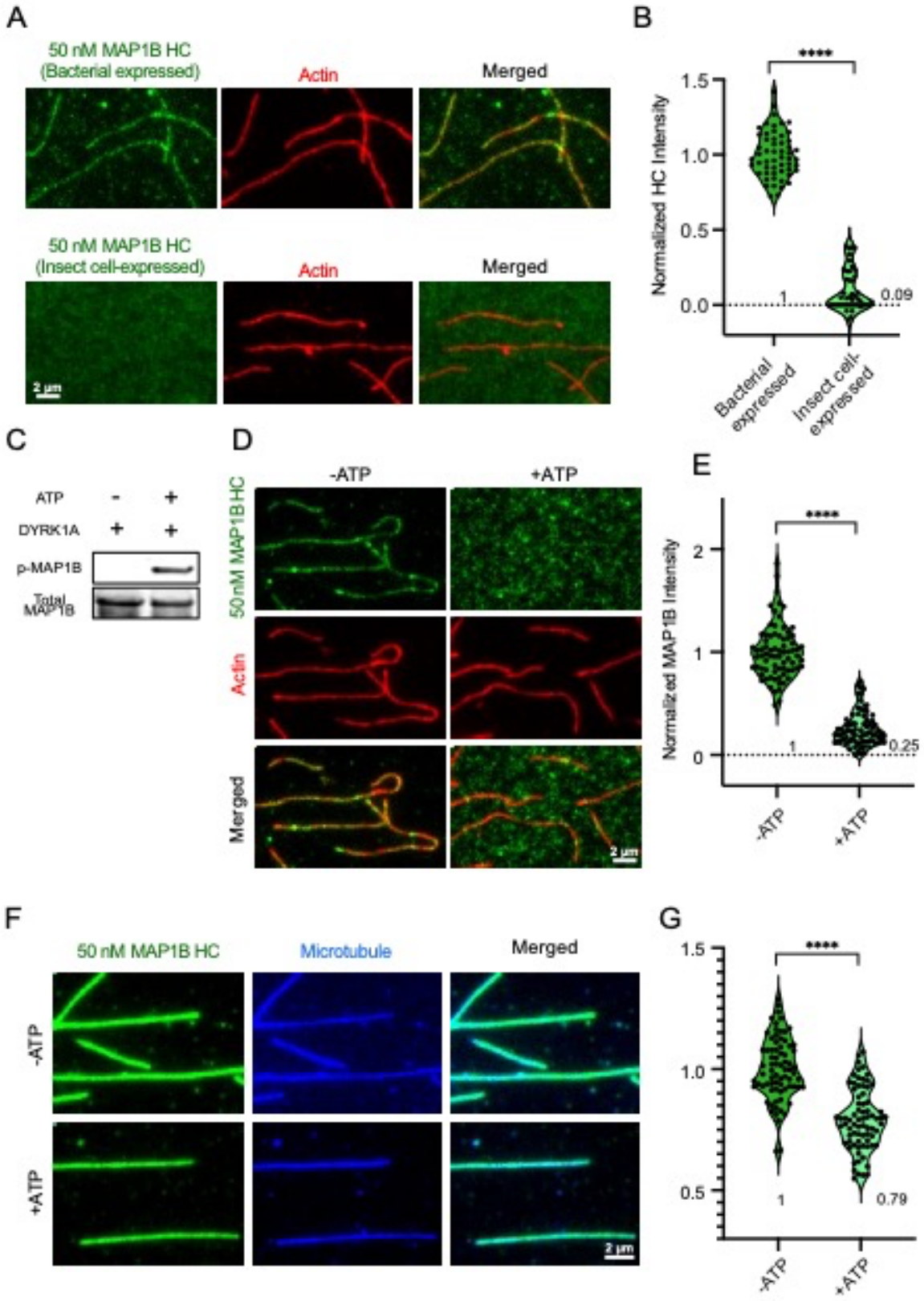
A
50 nM MAP1B HC
(Bacterial expressed)
Actin
Merged
50 nM MAP1B HC
(Insect cell-expressed)
Actin
Merged
2 µm
B
****
Normalized HC Intensity
1.5
1.0
0.5
0.0
1
0.09
Bacterial expressed
Insect cell-expressed
C
ATP - +
DYRK1A + +
p-MAP1B
Total MAP1B
D
-ATP
+ATP
50 nM MAP1B HC
Actin
Merged
2 µm
E
****
Normalized MAP1B Intensity
2
1
0
1
0.25
-ATP
+ATP
F
50 nM MAP1B HC
Microtubule
Merged
-ATP
+ATP
2 µm
G
****
1.5
1.0
0.5
1
0.79
-ATP
+ATP

Figure 4. Phosphorylation of MAP1B HC 1-1500 by DYRK1A regulates its affinity to actin. (A) TIRF-M images of bacterially expressed MAP1B HC 1-1500 (no phosphorylation) and insect cell-expressed MAP1B HC 1-1500 (with phosphorylation) on microtubules. (B) Quantification of bacterially expressed HC 1-1500 and insect cell-expressed MAP1B HC 1-1500, n=55 and 48 actin filaments, respectively, from 2 independent experiments, ****p<0.0001. (C) Western blot of phosphorylation of bacterially expressed strep-tagged MAP1B HC 1-1500 by DYRK1A in the absence or presence of 1mM ATP. The reaction mixtures were subjected to SDS-PAGE, followed by Western blot analysis with strep tag and Phospho-Threonine/Serine antibodies, n=3. (D) TIRF-M images of 50 nM of bacterially expressed MAP1B HC 1-1500 and DYRK1A in the absence or presence of 1mM ATP on actin filaments. (E) Quantification of fluorescence intensity of MAP1B HC 1-1500 in the presence of DYRK1a with and without 1mM ATP on actin filaments, n=76, 78 actin filaments, respectively, from 3 independent experiments, ****p<0.0001. (F) TIRF-M images of 50 nM of bacterially expressed MAP1B HC 1-1500 and DYRK1A in the absence or presence of 1mM ATP on microtubules. (G) Quantification of fluorescence intensity of MAP1B HC 1-1500 with and without 1mM ATP on microtubules, n=75 microtubules for each condition from 3 independent experiments, ****p<0.0001. All graphs show all datapoints. P-values were determined using an unpaired student's t-test.

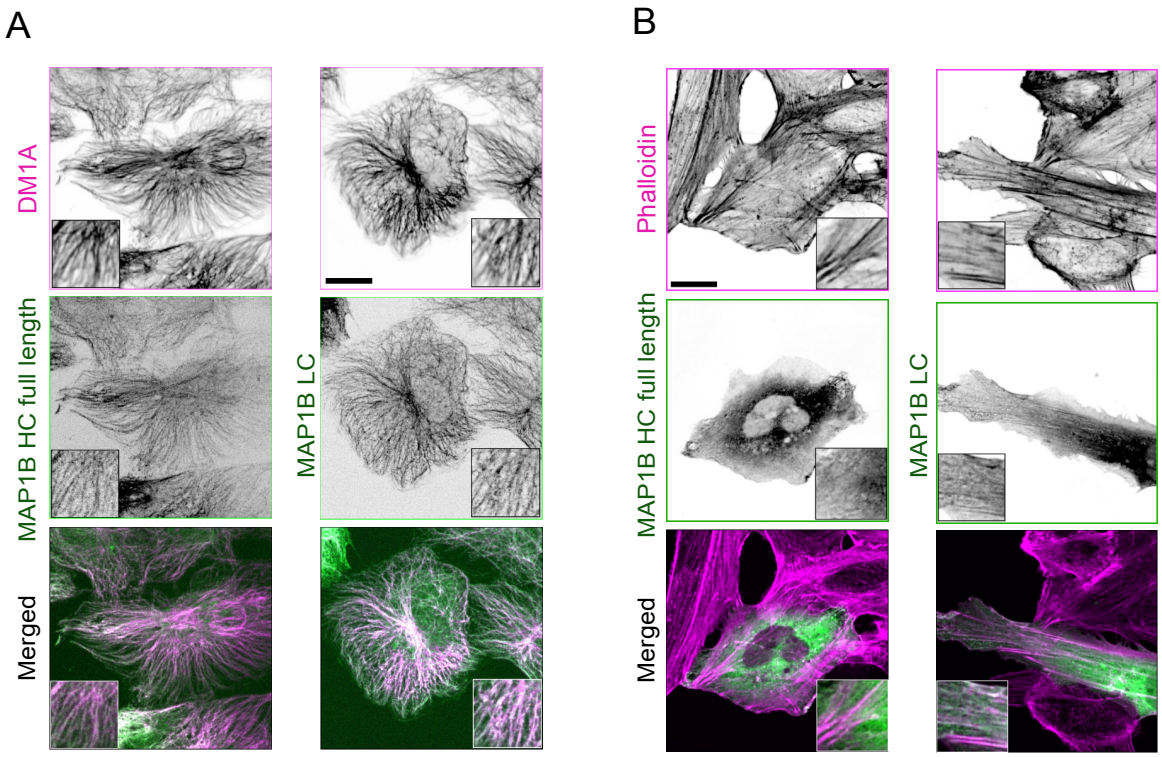
A
DM1A
MAP1B HC full length
Merged
MAP1B LC
B
Phalloidin
MAP1B HC full length
Merged
MAP1B LC

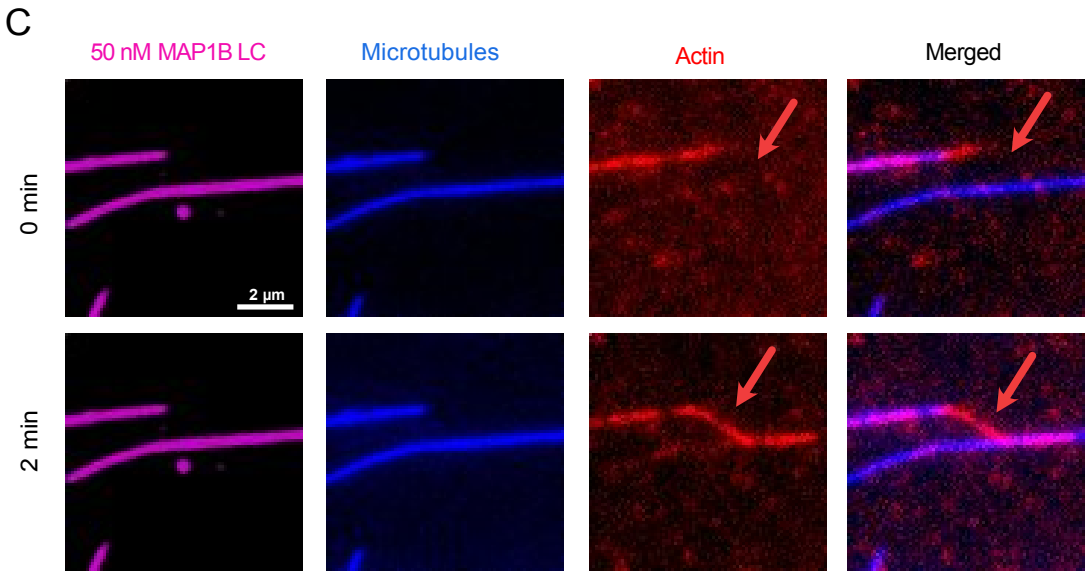
C
50 nM MAP1B LC
Microtubules
Actin
Merged
0 min
2 min
2 µm

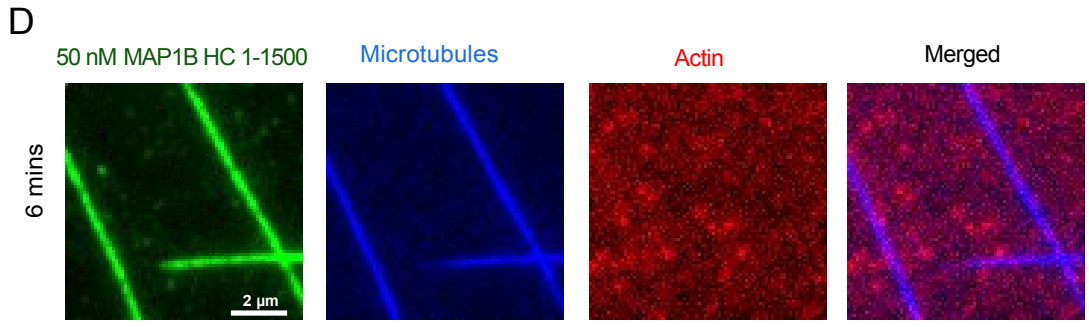
D
50 nM MAP1B HC 1-1500
Microtubules
Actin
Merged
6 mins
2 µm

Figure 5. LC binds to actin and directs F-actin polymerization on microtubules. (A) Confocal images of BEAS2B cells expressing superfolder-GFP tagged MAP1B HC or LC, immunostaining for tubulin. (B) BEAS2B cells expressing superfolder-GFP tagged MAP1B HC or LC, staining actin with phalloidin. Scale bar: 5 μm. Representative images from n = 2. (C) TIRF-M images of actin polymerization (red) on LC-bound microtubules from a time-course movie at 0 min (top) and 2 min (bottom). (D) TIRF-M images of the absence of actin polymerization (red) on HC-bound microtubules after 6 mins of actin polymerization. All graphs show all datapoints. P-values were determined using an unpaired student's t-test.

Both MAP1B HC full length binds to microtubules, but only LC binds to actin stress fibers *in vivo*

Using TIRF-M, we directly observed MAP1B HC and LC binding behaviors on microtubules and actin filaments. To confirm whether they behave the same in cells, we transiently transfected the lung epithelial cell line, BEAS2B, with MAP1B HC or LC and imaged their localization in cells using confocal microscopy. To maintain the integrity of microtubules and actin filaments' architecture, we employed two distinct fixation protocols. Paraformaldehyde fixation was chosen for better preservation of actin, while the methanol fixation method was preferred to maintain the structure of microtubules. We observed that both MAP1B HC and LC bind to microtubules within cells (figure 5A). Proteins expressed in mammalian cells are likely post translationally modified. Both HC and LC were able to robustly bind to microtubules. However, only the LC was able to bind on actin stress fibers (figure 5B). MAP1B HC showed a diffusive cytoplasmic

distribution in cells (figure 5B), which reconcile to the binding behaviors of purified recombinant MAP1B HC we have observed in TIRF-M actin binding assay *in vitro*.

MAP1B LC directs actin polymerization along microtubules.

Although many studies and our data have shown that the MAP1B LC binds to actin stress fibers in cells, the exact role and molecular mechanism of LC in cytoskeletal organization is unclear. We performed a dynamic actin polymerization assay and observed that the LC was able to bind actin and direct actin polymerization along microtubules (figure 5C). We mixed 50 nM LC and 1 μM G-actin monomers with 1 mM ATP and added the mixture to flow chambers with coverslips coated with immobile microtubules. Then we took a 2 min time-course movie to image polymerization using TIRF-M. We observed that MAP1B LC saturates microtubules and recruits actin to the lattice (figure 5C). Overtime, actin filaments were polymerized along microtubules through the interactions with MAP1B LC. We also observed that polymerized actin filaments that extended out from one end of the microtubule were subsequently docked on an adjacent microtubule, likely captured by MAP1B LC on that adjacent microtubule (figure 5C). MAP1B LC therefore not only guides actin to polymerize across LC-bound microtubules, but also facilitates actin filaments to dock and anchor to the adjacent microtubules when they are in close proximity. However, MAP1B HC 1-1500 did not recruit actin to the microtubule or facilitate actin polymerization (figure 5). Although non-phosphorylated MAP1B HC 1-1500 binds to actin filaments, it does not facilitate actin polymerization like MAP1B LC .

Discussion

MAP1B plays a key role in neuronal development. Mutations in MAP1B are correlated with the development of a variety of neurological diseases including Parkinson's, schizophrenia, and periventricular nodular heterotopia. Understanding the molecular mechanism of how MAP1B regulate actin, microtubule, and microtubule-based activity will give us more insight to its role in cytoskeletal organization during neuronal development. We have tested the microtubule binding ability of different epilepsy-associated mutant variants of MAP1B, revealing that the longest variant (MAP1B 1-1103) displayed robust binding due to the presence of the MTBD 639-747. Of the two short mutant variants, MAP1B 1-532 weakly binds microtubules, while the *de novo* mutant, MAP1B 1-303 does not bind to microtubules. All MAP1B HC constructs containing the MTBD 639-747 showed robust binding to microtubules, as well as MAP1B LC. However, single molecule assays using TIRF microscopy showed that both HC and LC bind strongly to microtubules, with LC displaying a more diffusive behavior due to interactions with C-terminal tubulin tails. The interaction of LC and C-terminal of tubulins protects microtubules from severing by Spastin. MAP1B HC also protects microtubules, but to a much lesser extent than LC. This might due to MAP1B HC being more statically bound to microtubules and spatially protecting the lattice, rather than competing for binding to C-terminal tails of tubulin with Spastin. Although previous studies have shown that MAPs differentially regulate motor proteins and selectively facilitate the motility of different kinesins (Lipka et al., 2016; Monroy et al., 2018, 2020), MAP1B seems to be a global inhibitor of many motor proteins. It inhibits kinesin-3, kinesin-4 and DDB from landing on the microtubules lattice. We also investigated the effect of MAP1B on actin. MAP1B LC and non-phosphorylated HC bind to actin filaments. However, MAP1B HC negatively regulates the

interaction between MAP1B LC and actin filaments by forming a HC-LC complex to mask the actin binding domain on LC. Moreover, we found that phosphorylation of MAP1B HC 1-1500 by DYRK1A leads to disassociation from actin. It decreases MAP1B HC 1-1500's affinity to actin drastically. However, the effects on microtubule binding were mild. In contrast, MAP1B LC's actin binding ability was not affected despite having post translational modifications in cells. Moreover, we found that MAP1B LC binds to actin monomers and direct actin polymerization over microtubules to crosslink these two cytoskeletons. MAP1B LC facilitates the unanchored polymerized actin filaments to dock on microtubules and keep these two cytoskeletons connected without being statically bound to actin filaments. Our data has also revealed how phosphorylation of MAP1B HC regulates its affinity to actin. DYRK1A is a key kinase that negatively regulates MAP1B HC's affinity to actin filaments. Overall, we have conducted an in-depth study of MAP1B, both HC and LC, and characterized the molecular mechanism of mediating actin and microtubule crosstalk.

Materials and Methods

Molecular biology

The cDNA for protein expression in this study were as follows: mouse MAP1B (Transomic #BC138033), mouse KIF21A, human KIF1A (aa 1-393; Addgene #61665), human DCX (Addgene #83929), human Tau-2N4R (Addgene #16316). MAP1B HC 1-303, HC 1-532, HC 1-1103, HC 1-1500 and HC MTBD proteins were cloned in frame using Gibson cloning into a pET28 vector with a N-terminal Strepll-Tag, mScarlet or a superfolder GFP (sfGFP) cassette. KIF1A (1-393) and MAP1B

LC proteins was cloned in frame using Gibson cloning into a pET28 vector with an C-terminal mScarlet-Strepll or sfGFP-Strepll cassette. MAP1B HC full length and KIF21A 1-930 proteins were cloned in frame using Gibson cloning into a pACEBAC vector with C-terminal sfGFP-Strepll and mScarlet-Strepll cassette, respectively. HC 1-1500 were cloned in frame using Gibson cloning into a pACEBAC vector with a N-terminal mScarlet-Strepll cassette.

Protein expression and purification

For bacterial expression of sfGFP-MAP1b 1-303, sfGFP-MAP1B 1-532, sfGFP-MAP1B 1-1103, sfGFP-MAP1B 1-1500, mScarlet-MAP1B 1-1500 and MAP1B LC 2203-2464-sfGFP, BL21 cells were grown at 37°C until reached O.D 0.6-0.8, and protein expression was induced with 0.1mM IPTG. Cells were grown overnight at 18°C and harvested. BL21 cells expressing Dyrk1AΔC(1-499) were grown at 37°C until reached O.D 0.6-0.8, and protein expression was induced with 0.2mM IPTG and allowed grown for 3 hours at 30°C and harvested. The cell pellets were rinse with PBS and resuspended in lysing buffer (50mM Tris, 150mM K-acetate, 2mM $MgSO_4$, 2mM EGTA, 10% glycerol, pH8.0), supplemented with 1mM DTT and 1mM PMSF and PI mix. Cells were lysed by Emulsiflex and clarified by centrifugation at 11,000 xg for 20 minutes. Clarified lysate was passed through Strep-Tactin XT column for one hour. Protein was washed with lysis buffer for three column volume and then eluted off from the column with 100mM D-biotin in lysis buffer. The protein was further purified with ion exchange column (HiTrap Q or HP) or size exclusion column (Suprose-6 GE Health).

For insect cells expression of mScarlet-MAP1B 1-1500 and MAP1B 1-2202-sfGFP, sf9 cells were grown in shaker flask to about 2 million/ml and infected at 1:100 ratio of virus and allowed

protein expression for 60 hours. Cells were harvested and rinsed with PBS. The cell pellet was resuspended in lysis buffer (50mM Tris, 150mM K-acetate, 2mM $MgSO_4$, 2mM EGTA, 10% glycerol, pH8.0), supplemented with 1mM DTT and 1mM PMSF and PI mix, and then lysed in Dounce homogenizer with 1% Triton-X100. The lysate was centrifuged at 11,000xg for 20 minutes. Clarified lysate was passed through Strep-Tactin XT column for one hour. Protein was washed with lysis buffer for three column volume and then eluted off the column with 100mM D-biotin in lysis buffer. The protein was further purified with ion exchange column (HiTrap Q or HP) or Suprose-6 (GE Health) size exclusion column.

Kinase Assay

In vitro kinase assay was perform with bacterial expressed mScarlet-MAP1B1-1500 and sfGFP-Dyrk1AΔC in assay buffer(90mM SRP, 50mM K-acetate, 2mM EGTA, pH 7.6), supplemented with k-casein, BSA, 10uM Taxol, 1uM phalloidin. 500nM of bacterial expressed mScarlet-MAP1B HC 1-1500 and sfGFP-Dyrk1AΔC were incubated in final volume of 50uL with or without 2mM ATP at 37°C for 30 minutes.

Preparation of Microtubules

A mixture of native tubulin, biotin-tubulin, and fluorescent-tubulin purified from porcine brain (~10:1:1 ratio) was assembled in BRB80 buffer (80 mM PIPES, 1 mM MgCl2, 1 mM EGTA, pH 6.8 with KOH) with 1 mM GTP for 15 min at 37 °C, then polymerized MTs were stabilized with 20 µM Taxol. Microtubules were pelleted over a 25% sucrose cushion in BRB80 buffer to remove unpolymerized tubulin. For subtilisin removal of the C-terminal tubulin tails, the assembled MTs

were digested with 200 μg/mL subtilisin for 1 hour at 37°C. The digestion was terminated by addition of PMSF and the digested MTs were centrifuged over a 25% sucrose cushion to remove the subtilisin protease before use.

TIRF Microscopy

Flow chambers containing immobilized microtubules were assembled as described (McKenney et al., 2014). Imaging was performed on a Nikon Eclipse TE200-E microscope equipped with an AndoriXon EM CCD camera, a × 100, 1.49 NA objective, four laser lines (405, 491, 568, and 647 nm) and Micro-Manager software43. All binding assays of MAPs on microtubule experiments were performed in assay buffer (90 mM Hepes pH 7.4, 150 mM K-acetate, 2 mM Mg- acetate, 1 mM EGTA, and 10% glycerol) supplemented with 0.1 mg/mL biotin- BSA, 0.5% Pluronic F-168, 10uM Taxol, and 0.2 mg/mL κ-casein (Sigma). All binding assays of MAPs on actin filaments were performed in assay buffer (90 mM Hepes pH 7., 150 mM K-acetate, 2 mM Mg- acetate, 1 mM EGTA, and 10% glycerol) supplemented with 0.1 mg/mL biotin- BSA, 0.5% Pluronic F-168, 10 μM Taxol, 0.1 mM of Phalloidin, and 0.2 mg/mL κ-casein (Sigma).

ATP concentrations are indicated in the legends. Motility data was analyzed by kymograph analysis in ImageJ (NIH) to determine landing rates of processive motors.

For fluorescent intensity analysis, a segmented line was drawn on microtubule or actin filaments, and the mean intensity value was recorded. The segmented line was then moved adjacent to the microtubules or actin filaments of interest and a local background vale was recorded. The background value was subtracted from the value of interest to give the background corrected intensity.

Cell Culture and Immunocytochemistry

BEAS-2B cells were used for cell imaging experiments. They were maintained in Dulbecco's modified Eagle's medium (DMEM, Life Technologies), supplemented with 10% fetal bovine serum (FBS), 50units/mL of penicillin and 50 μg/mL of streptomycin. All cell cultures were maintained in a 95% air/ 5% CO_2 atmosphere at 37°C. The cell lines were routinely confirmed to test negative for mycoplasma contamination.

The expression vectors used in this study were pEGFP-MAP1B HC 1-2202 and pEGFP- MAP1B LC 2203-2464. Transfections were performed by using the Lipofectatmine 20000 reagent kit (Invitrogen) according to manufacturer's instructions. Cells were generally transfected for 8 hours with 1 μg plasmids when the density reached ~80% confluency. Cells were fixed with 4% PFA or ice-cold methanol for 10 minutes at room temperature or at -30°C. Fixed cells were washed with PBS and permeabilized in 0.5% Triton X-100 for 10 minutes. Coverslip was washed with PBS and block with 4% BSA for one hour at room temperature. Cultures Were then incubated with DM1A antibody at a concentration of 1:500 for 2 hours at room temperature. Secondary antibodies were used at a concentration of 1:1000 for anti-DM1A and 1:1000 for Alexa-647 conjugated phalloidin for 1 hours in room temperature. Cells were washed 3 times in PBS after incubation with secondary antibodies, and then mounted onto a microscope slide with ProLong™ Gold Antifade Mountant (Invitrogen), and then examined by spinning disk confocal microscopy.

Confocal microscopy

The spinning disk confocal was performed on an inverted research microscope Eclipse Ti2-E with the Perfect Focus System (Nikon), equipped with a Plan Apo 60x NA 1.40 oil objective, a rest X-Light V3 spinning disk confocal head (Crest-Optics), a Celesta light engine (Lumencor) as the light source, a Prime 95B 25MM sCMOS camera (Teledyne Photometrics) and controlled by NIS elements AR software (Nikon). The fluorescent images for BEAS-2B cells were collected over a stack of vertical z-sections across the entire cell ~4 μm thickness. The final fluorescent images shown in the main text and figures are based on the z-averaged images by using Fiji software (https://fiji.sc/)

Statistical analysis

All statistical tests were performed with unpaired t-tests.

Supplemental Figures

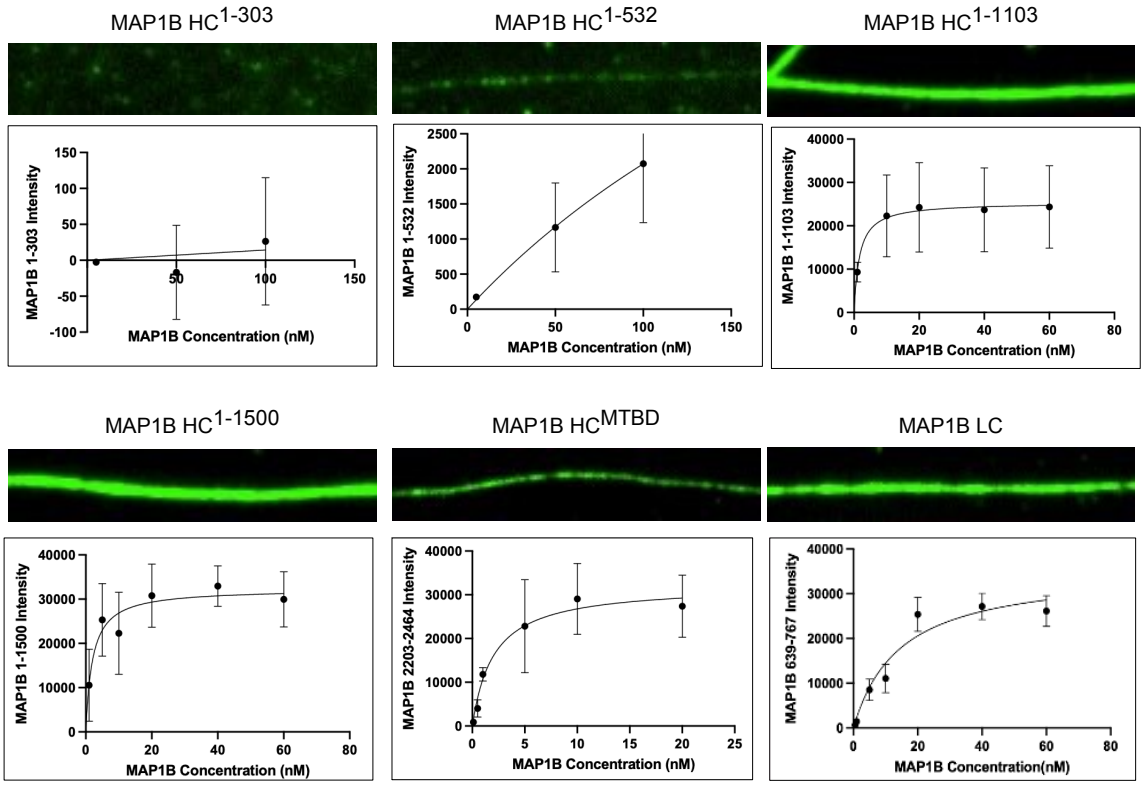

Supplementary Figure 1. Saturation curve of MAP1B HC, truncations variants, and LC. TIRF-M images of 100nM of MAP1B HC 1-303 and MAP1B HC 1-532, and 5nM of MAP1B HC 1-1103, MAP1B HC 1-1500, MAP1B HC microtubule binding domain and MAP1B LC bound to microtubules. The corresponding quantification of fluorescence intensity of microtubule-bound MAP1B plotted again concentration (MAP1B 1-303 does not bind to microtubule. n>130 microtubules for each 5nM , 50nM, 100 nM concentrations from 3 independent experiments. MAP1B 1-532: KD = 74.38 nM n>130 microtubules for each 5nM , 50nM, 100 nM, 500 nM concentrations from 3 independent experiments. MAP1B 1-1103: KD= 1.58. n>130 microtubules for each 0.5 nM, 1 nM , 5 nM, 10 nM, 20 nM, 40 nM concentrations. MAP1B 1-1500: KD= 3.56.

n>130 microtubules for each 0.5 nM, 1 nM , 5 nM, 10 nM, 20 nM, 40nM, 60nM concentrations from 3 independent experiments. MAP1B MTBD: KD= 11.54 . n>130 microtubules for each 0.5 nM, 1 nM, 5 nM, 10 nM, 20 nM, 40 nM, 60nM concentrations from 3 independent experiments. MAP1B LC: KD= 1.54 . n>130 microtubules for each 0.1 nM, 0.5 nM, 1 nM, 5 nM, 10 nM, 20 nM concentrations from 3 independent experiments. All graphs show all datapoints. P-values were determined using an unpaired student's t-test.

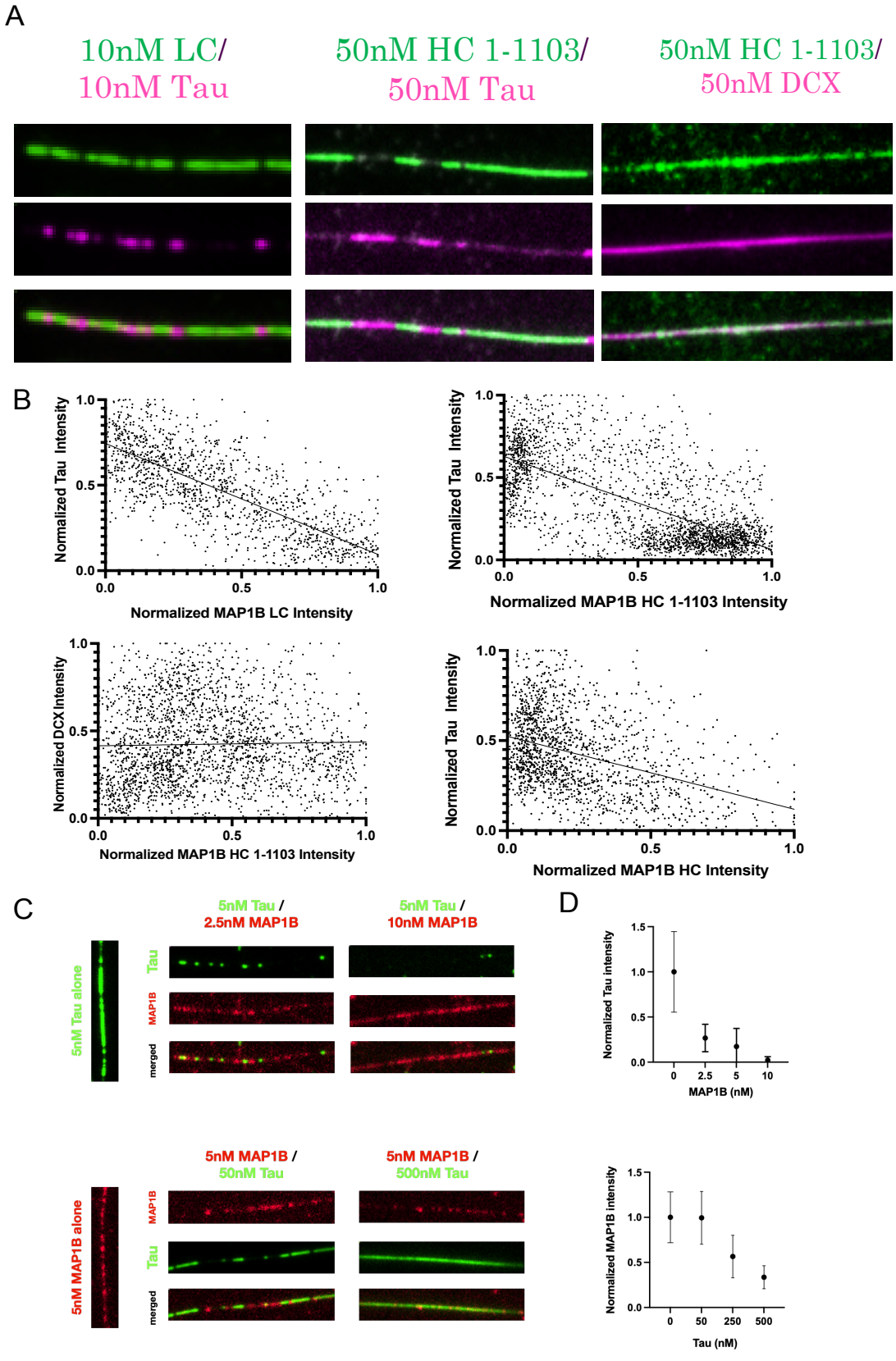
A
10nM LC/
10nM Tau
50nM HC 1-1103/
50nM Tau
50nM HC 1-1103/
50nM DCX
B
Normalized Tau Intensity
Normalized MAP1B LC Intensity
Normalized MAP1B HC 1-1103 Intensity
Normalized DCX Intensity
Normalized MAP1B HC Intensity
C
5nM Tau alone
5nM Tau /
2.5nM MAP1B
5nM Tau /
10nM MAP1B
Tau
MAP1B
merged
5nM MAP1B alone
5nM MAP1B /
50nM Tau
5nM MAP1B /
500nM Tau
D
Normalized Tau intensity
MAP1B (nM)
Normalized MAP1B intensity
Tau (nM)

Supplementary Figure 2. Analysis of the effects of MAP1B on other MAPs. (A) TIRF-M images of binding assays of 10 nM MAP1B LC-sfGFP and mScarlet-Tau on microtubules, sfGFP-MAP1B HC 1-1103 and mScarlet-Tau on microtubules, sfGFP-MAP1B HC 1-1103 and mScarlet-DCX on microtubules. Both MAP1B HC 1-1103 and LC segregate Tau into homotypic patches, while DCX does not exclude MAP1B HC1-1103. (B) Graph displaying individual xy pairs per pixel for MAP1B LC, MAP1B HC 1-1103, or and MAP1B HC full length intensity versus tau intensity on the microtubules, fit with a linear regression. Pearson correlation coefficient r = -0.75 (n=1357 xy pairs from 10 microtubules, r = -0.68 (n=2317 xy pairs from 10 microtubules), r= -0.39 (n = 1545 xy pairs from 10 microtubules), respectively. Graph displaying individual xy pairs per pixel for MAP1B 1-1103 intensity vs DCX intensity on the microtubules. Pearson correlation coefficient r = 0.02 (n=2254 xy pairs). (C) Top panel: TIRF-M images of tau on microtubules in the absence and presence of increasing concentrations of endogenous MAP1B HC. Bottom panel: TIRF-M images of endogenous MAP1B HC on the microtubules in the absence or presence of increasing concentrations of tau. (D) Quantification of tau fluorescence intensity on microtubules plotted as a function of MAP1B concentration (n=100 microtubules) and MAP1B fluorescence intensity on microtubule plotted as a function of tau concentration (n=100 microtubules). All graphs show all datapoints. P-values were determined using an unpaired student's t-test.

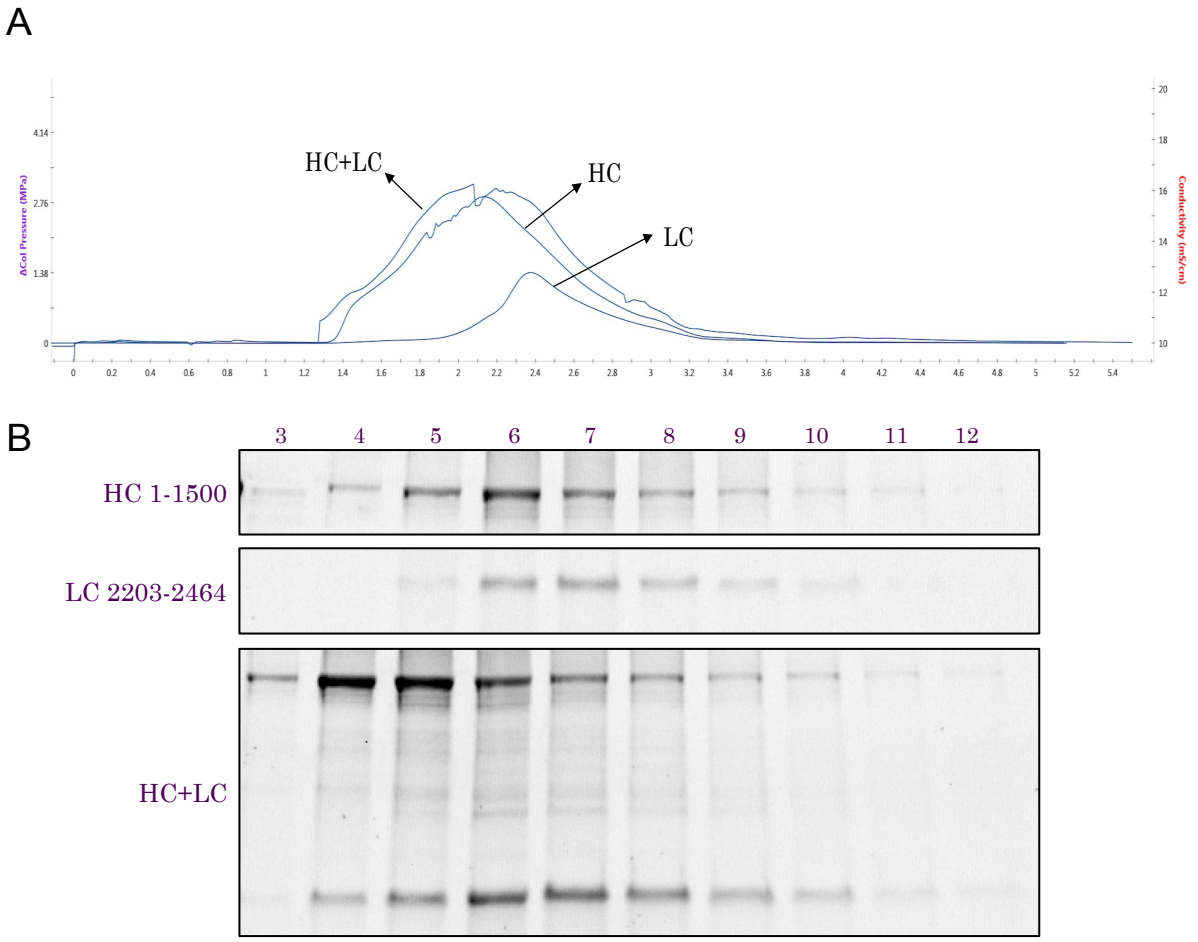

Supplementary Figure 3. Analysis of MAP1B HC-LC complex. (A) Elution profile graph of MAP1B HC 1-1500 alone, MAP1B LC alone, and HC 1-1500 and LC combined from Suporose6 size exclusion chromatography. (B) SDS-PAGE gel of fractions of HC 1-1500, MAP1B LC, and HC 1-1500 and LC mixture from Suporose6 size exclusion chromatography. MAP1B HC 1-1500 started to elute at fractions 3, while LC started at fractions 4-5. In the HC-LC mixture run, both HC and LC eluted two fractions earlier than the LC alone run, indicating HC-LC forms a complex.

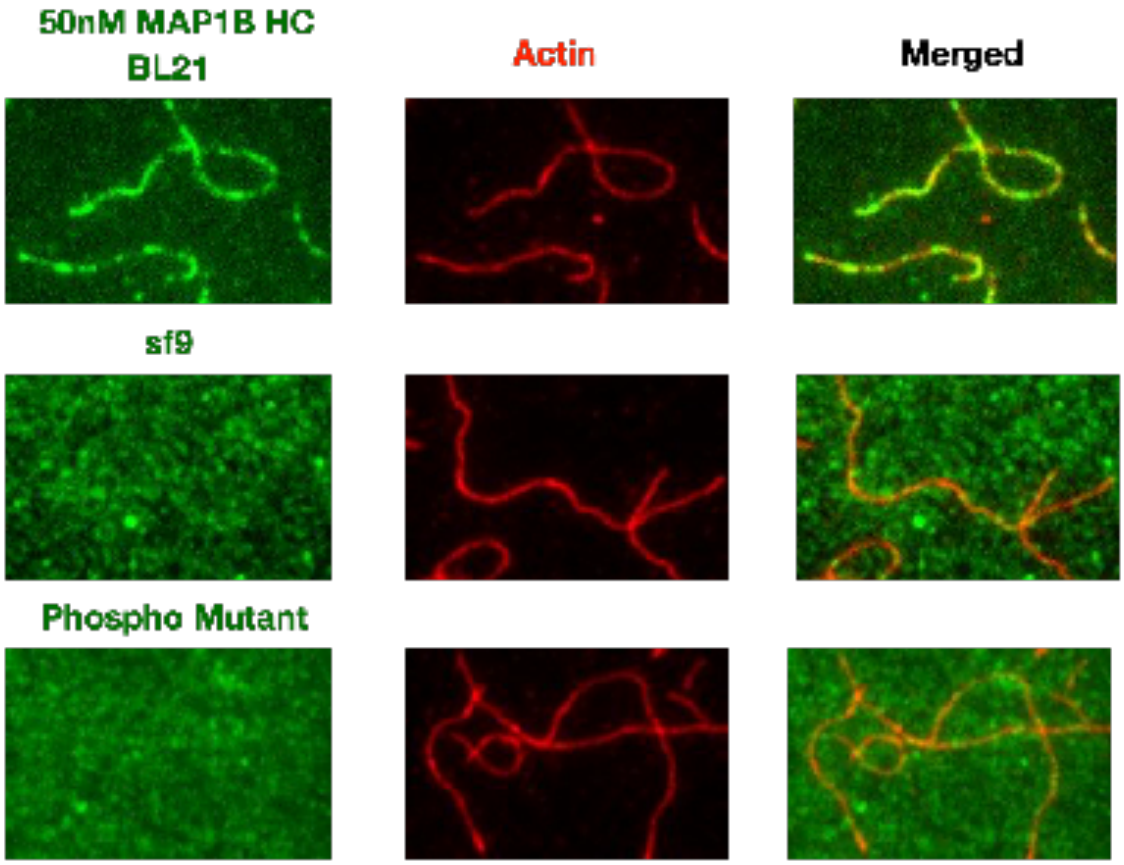

Supplementary Figure 4. Phospho-mutant of MAP1B HC 1-1500 does not bind to actin filaments. TIRF-M images of bacterial expressed 50 nM MAP1B HC 1-1500, insect cell-expressed MAP1B HC 1-1500, insect cell-expressed MAP1B HC 1-1500 phospho-mutant (S1260A, S1265A, S1390A, S1395A).

Chapter 3: Co-Authorship Contributions and Unpublished Findings

I joined the McKenney and Ori-McKenney labs (MOM lab) in my junior year of undergrad. I first worked with a grad student in the lab to investigate the relationship between microtubule-associated proteins and motor proteins. Our paper "Competition between microtubule-associated proteins directs motor transport" was published Nature Communications in 2018. In cells, both microtubule-associated proteins (MAPs) and motor proteins simultaneously converge on the microtubule. However, the coordination of binding activities of non-motor MAPs and their role in balancing and directing motor transport was unclear at the time. This paper focused on the interplay between MAP7 and Tau, which have opposite functions *in vivo*. We observed that MAP7 and Tau compete for binding to microtubules. Our data provided a mechanism by which MAP7 displaced Tau from the microtubule lattice. In addition, MAP7 enhanced kinesin-based transport in living cells and strongly recruited kinesin-1 to microtubules *in vitro*. This demonstrated that MAP7 directly enhances motor movement, indicating a novel mechanism of regulation by a MAP. Importantly, both MAP7 and Tau inhibit kinesin-3 but have no impact on cytoplasmic dynein, indicating how different MAPs selectively control specific classes of motors. These findings provided a general principle for how MAP competition influences microtubule lattices, thereby determining the appropriate distribution and balance of motor activity within cells. For this paper, I cloned a variety of genes into vectors for protein expression in bacteria or insect cells. I then expressed these proteins and purified them using a range of different methods, including different affinity columns and gel filtration columns. I therefore have ample experience in cloning, protein expression and purification, and size exclusion chromatography. These skills

were valuable as they enable me to conduct biochemical experiments using purified proteins and in vitro reconstitution system approaches during my later graduate study.

I continued to work in the Ori-McKenney lab as a junior specialist then as a graduate student after obtaining my bachelor's degree from UC Davis. My initial project was to understand how one microtubule-associated protein, tau, forms aggregates and becomes neurotoxic upon phosphorylation by a range of kinases. I was working on determining the cooperation and competition between three kinases in particular: Dyrk1A, GSK3β, and Akt. I produced phosphomimetic and phosphomutant versions of tau at different phosphorylation sites and I expressed and purified Dyrk1A, GSK3β, and Akt to see how their modifications differentially affected tau function. I performed kinase assays to determine how the addition of different kinases affected its binding behavior. Overall, we saw that Dyrk1A determines whether and how further phosphorylation of tau can occur, and therefore dictates whether tau is phosphorylated by a neurotoxic kinase (GSK3β) or a neuroprotective kinase (Akt).

Alzheimer Disease (AD) is the most common cause of dementia in adults. The appearance of neurofibrillary tangles (NFTs) in the brain is one of the hallmarks of AD, and the NFTs may play a causative role in the disease. NFTs consist of hyperphosphorylated tau aggregates. However, the underlying mechanism of tau hyperphosphorylation still remains unknown. Some kinases that phosphorylate tau promote NFT formation, while other kinases play opposing roles. There are more than 40 phosphorylation sites that have been identified in tau aggregates (Kimura et al., 2016).

GSK3β is a major kinase that heavily phosphorylates tau at more than six sites (Avila et al., 2012; Wang & Mandelkow, 2016), and its activity is thought to promote tau toxicity. However, some studies suggest that site-specific phosphorylation of tau is not always pathological (Ittner et al., 2016; Schneider et al., 1999). Akt is a kinase involved in neuronal regeneration that predominantly phosphorylates tau at S214 (3,5)(Song et al., 2012; Yu & Koh, 2017), and S214 phosphorylation has been reported to have a protective effect against tau assembly in to NFTs (Schneider et al., 1999).

Many individuals with Down Syndrome (DS) show early onset of AD, but the underlying mechanism remains unknown(Liu et al., 2008; Ryoo et al., 2007). Both DS and AD patients have common pathological hallmark, which is the presence of NFTs consisting of hyperphosphorylated tau protein aggregates. Dyrk1A is a kinase located in the DS critical region in Chromosome 21, and it predominately phosphorylates tau at T212. Previous studies have shown that high levels of phosphorylation of tau T212 are found in NFTs in both DS and AD patient brains (Ryoo et al., 2007). Overexpression of human DYRK1a in transgenic mice showed a significant increase of Tau phosphorylation at T212 (Liu et al., 2008; Ryoo et al., 2007). The high level of Dyrk1A expression might contribute to hyperphosphorylation of tau and lead to the formation of NFTs.

We found that tau T212 phosphorylation by Dyrk1A facilitated further tau phosphorylation by GSK3β, and prevented S214 phosphorylation by Akt. We hypothesize that DYRK1a might affect tau aggregation by modulating its phosphorylation by Akt and GSK3β, changing its microtubule binding affinity and accelerating NFT formation.

Dyrk1A efficiently phosphorylates tau to generate a single phosphorylated form *in vitro* within 40mins. To investigate the link between Dyrk1A and tau phosphorylation at T212 *in vitro*, we first performed a kinase assay time-course and analyzed the results using Phos-Tag gels, which interact with phosphate groups to cause large shifts in apparent molecular weight for phosphorylated proteins (Figure 1).

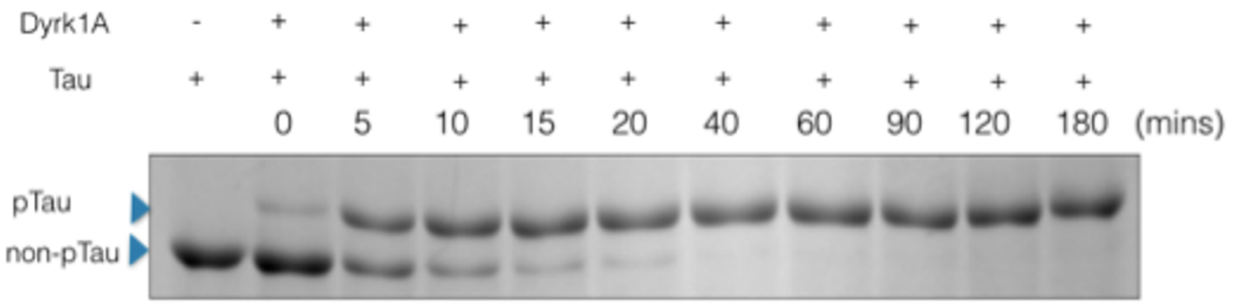

Figure 1. *In-vitro* Time-course kinase assay of Tau phosphorylation by DYRK1a using a Phos-Tag gel. Top band is phosphorylated Tau and bottom band is non-phosphorylated Tau.

Since the Phos-Tag gels separate proteins based on their phosphorylation status, a protein that was phosphorylated at multiple sites would migrate much slower than the same protein phosphorylated at only one site, and multiple bands above the control band should be observed. Since only one such band was observed for tau, we conclude that Dyrk1A predominantly phosphorylated tau at one site, which is likely T212 based on prior literature and our experiments with a phospho-specific antibody against p-T212.

Dyrk1A primes tau for further phosphorylation by GSK3β. To determine if phosphorylation of tau-T212 by DYRK1a facilitates further tau phosphorylation by GSK3β, we performed a kinase assay using purified GSK3β, either with or without pre-incubation of tau with

Dyrk1A. We used a Western blot with an anti-pTauS199/202 (GSK3β phosphosites) antibody to compare the phosphorylation level of tau. We observed that pre-incubation of tau

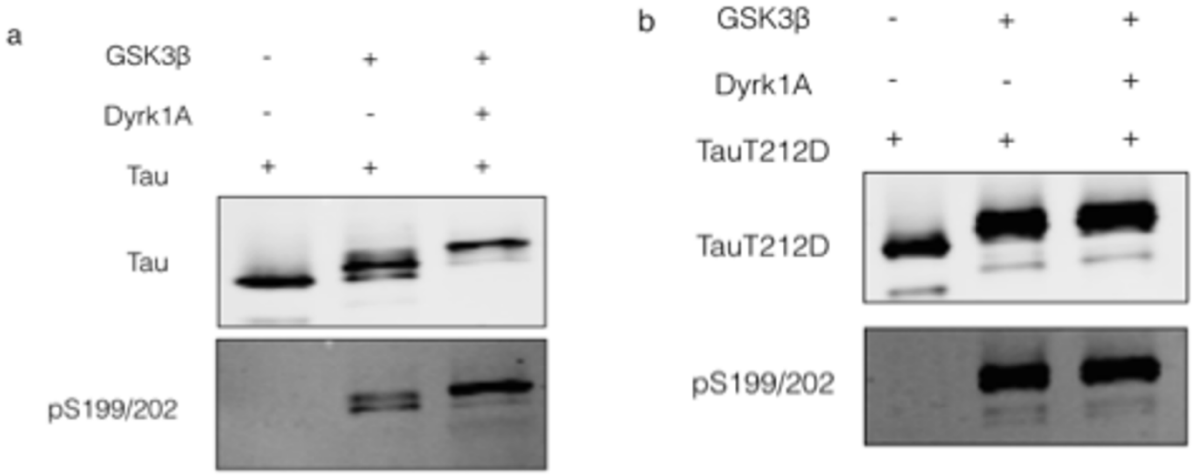

Figure 2. Phosphorylation of TauT212 by Dyrk1A promotes further phosphorylation of Tau by GSK3β. a) *In vitro* Western blot of phosphorylation of Tau by before (lane 2) and after (lane 3) pre-incubation with Dyrk1A. b) Western blot of phosphorylation of Tau T212D mutant by GSK3β before (lane 2) and after (lane 3) pre-incubation with Dyrk1A. The reaction mixtures were subjected to SDS-PAGE, followed by Western blot analysis with Tau and phosphor-Ser-199/202-Tau (pS199/202) antibodies.

with Dyrk1A led to increased phosphorylation by GSK3β (Figure 2a). We also performed the kinase assay using tau with a T212D mutation to mimic Dyrk1A-mediated phosphorylation. The signal intensity of phosphorylated tau for Dyrk1A preincubated and non-preincubated conditions were very similar, suggesting that phosphorylation at T212 is responsible for Dyrk1A's priming effect (Figure 2b).

Phosphorylation of tau T212 by Dyrk1A prevents Akt from phosphorylating tau at S214.

To investigate the relationship between Dyrk1A and Akt's ability to phosphorylate Tau S214, we performed kinase assays using purified tau, Dyrk1a and Akt proteins. We measured phosphorylation by Western blot using a pTauS214 antibody. When tau was incubated only with Akt, we observed a strong tau phosphorylation signal in the blot. However, when tau was first pre-incubated with Dyk1A, we did not detect phosphorylation, indicating that phosphorylation of tau by Dyrk1A inhibits phosphorylation two sites over at S214 by Akt (Figure 3a).

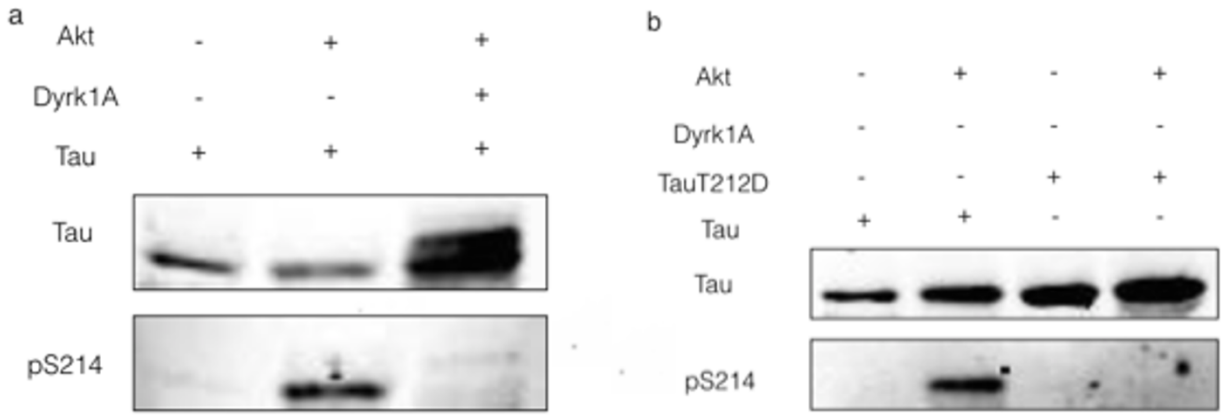

Figure 3. phosphorylation of tau at T212 by DYRK1A prevents Akt from phosphorylating tau at S214. a) *In vitro* Western blot of phosphorylation of tau by Akt before (lane 2) and after (lane 3) pre-incubation with DYRK1A. b) Western blot of phosphorylation of tau T212D mutant by Akt. The reaction mixtures were subjected to SDS-PAGE, followed by Western blot analysis with total tau and phosphor-Ser-214-Tau (pS214) antibodies.

We also performed the kinase assay using the tau T212D mutant and observed that the mutation also blocked phosphorylation at S214, consistent with the idea that phosphorylation of tau at T212 by Dyrk1A is responsible for the inhibitory effect (Figure 3b).

While I was working on my tau phosphorylation project, I also contributed to another project focused on the tau protein. The resulting paper, “Microtubules gate tau condensation to spatially regulate microtubule functions” was published in Nature Cell Biology in 2019. Tau aggregation into the insoluble NFT fibrils described above is a hallmark of AD and similar dementias. However, the non-pathologic, physiological state of Tau molecules within cells was still unclear. We used single-molecule imaging to directly observe that the microtubule lattice plays a role in regulating the reversible self-association of tau. This leads to localized and dynamic clustering of tau molecules on the microtubule lattices. These tau condensates act as selectively permissible barriers, influencing the activity of microtubule-severing enzymes and controlling the movement of molecular motors along the microtubules. The data suggests that reversible self-association of tau molecules, controlled by the microtubule lattice, is a crucial mechanism underlying the biological functions of tau. Furthermore, this process of tau oligomerization appears to be a common characteristic shared between the normal physiological form of tau and the pathological forms. For this paper, I cloned, expressed and purified a variety of tau truncations. In addition, I learned how to perform single-molecule TIRF assays to observe how tau molecules form cooperative self-assemblies that we termed “condensates,” and to analyze if and how different tau truncations could co-localize with the condensates.

When I was working on my thesis project, “Biochemical dissection of MAP1B complex”, I also contributed to another project to investigate how different microtubule-associated proteins (MAPs) influence the motility of kinesin and dynein motors. Our paper “A Combinatorial MAP Code Dictates Polarized Microtubule Transport” was published in Developmental Cell in 2020. In eukaryotic cells, the distribution of intracellular components is essential for proper function, and this distribution is often achieved through regulated active transport that is driven by molecular motors moving along microtubules. While we understand that both intrinsic factors within the motors and extrinsic factors in the cellular environment can influence motor activity, the mechanisms governing the overall distribution of activated motor-cargo complexes within cells was unclear. In this paper, we used in vitro reconstitution of purified motor proteins and non-enzymatic MAPs to investigate how MAPs differentially regulate motor proteins. We found that MAPs display distinct effects on the motility of three main classes of transport motors: kinesin-1, kinesin-3, and cytoplasmic dynein. This paper revealed how combinations of different MAPs affect motor functions. In addition, we found that MAP9 acts as a positive regulator kinesin-3 motility. Based on these findings, we proposed a general 'MAP code', which can bias motor movement along microtubules and help understanding the complex intracellular transport within highly polarized cells like neurons. For this paper, I cloned, expressed, and purified different MAPs including DCLK, DCX, Map2, Tau, MAP7 and Map9 from bacterial cells or insect cells. I also performed a number of immunostaining experiments in neurons cultured from mouse embryonic brains to observe the localization patterns of these MAPs.

While I was working on my thesis project, I also contributed to another project to investigate how the autophosphorylation of doublecortin-like kinase 1 (DCLK1) control its microtubule binding. Our paper “Autoregulatory control of microtubule binding in doublecortin-like kinase 1” was published in eLife in 2021. The microtubule-associated protein doublecortin-like kinase 1 (DCLK1) is an important therapeutic target due to its high expression levels in various cancers. However, the physiological roles of its kinase activity and its regulation were unclear. We investigated how DCLK1's kinase activity affects its interaction with microtubules. We found that DCLK site-specific autophosphorylation within its C-terminal tail regulates its kinase activity and microtubule binding affinity. This phosphorylation in the C-terminal tail prevents excessive phosphorylation within the microtubule-binding domain. When the C-terminal tail is removed or when the phosphorylation site is mutated, this leads to higher level of phosphorylation within the doublecortin microtubule-binding domains, resulting in disruption of the binding of DCLK1 to microtubules. Our data revealed how site-specific autophosphorylation of DCLK1 has a profound impact on its interaction with microtubules. These results suggested that DCLK1 can modulate its kinase activity to tune its affinity for microtubules. These findings provided crucial molecular insights that can guide future therapeutic strategies related to DCLK1's role in cancer development and progression. For this paper, I expressed and purified DCLKΔC and mutant proteins. I performed kinase assays of DCLK wildtype, DCLKΔC and mutant variants, and examined their microtubule binding affinity using TIRF-M, analyzed data and participated in writing the manuscript.

When I was working on my thesis project, I also contributed to another project to investigate the effects of tau envelop formation on microtubule lattice. Our paper “Microtubule lattice spacing governs cohesive envelope formation of tau family proteins” was published on Nature chemical biology in 2022. The data revealed that tau envelopes form cooperatively and locally affect the spacing of tubulin dimers within the microtubule lattice. Envelope formation leads to a compaction of lattice, while expanding the lattice results in the disassembly of tau envelopes. We examined other members of the tau protein family: MAP2, which also forms envelopes and actively compacts the lattice, and MAP4, which does not exhibit this behavior. These envelopes differentially affect the movement of motor proteins, indicating that tau family members are able to create distinct functional regions on the microtubule lattice. The study concluded that the interconnected relationship between lattice spacing and cooperative envelope formation by MAP2 and tau provides the molecular basis for spatially regulating microtubule-based processes. For this paper, I cloned, expressed and purified MAP4 WT and MAP4 mutants. Using TIRF microscopy, I tested whether MAP4 and MAP4-pseudo-Tau-hydrophobic mutants can form “condensates” or “envelopes” like MAP2 and tau as they were all evolved from the same protein family. I also performed single molecule assay to investigate whether MAP4 can regulate kinesin and dynein motility like tau and MAP2. I analyzed data, wrote methods, and reviewed and edited the manuscript.

Reference

Avila, J., León-Espinosa, G., García, E., García-Escudero, V., Hernández, F., & Defelipe, J. (2012). Tau phosphorylation by GSK3 in different conditions. In *International Journal of Alzheimer's Disease*. https://doi.org/10.1155/2012/578373

Bianchi, S., Van Riel, W. E., Kraatz, S. H. W., Olieric, N., Frey, D., Katrukha, E. A., Jaussi, R., Missimer, J., Grigoriev, I., Olieric, V., Benoit, R. M., Steinmetz, M. O., Akhmanova, A., & Kammerer, R. A. (2016). Structural basis for misregulation of kinesin KIF21A autoinhibition by CFEOM1 disease mutations. *Scientific Reports*, *6*. https://doi.org/10.1038/srep30668

Bloom, G. S., Luca, F. C., & Vallee, R. B. (1985). Identification of High Molecular Weight Microtubule-Associated Proteins in Anterior Pituitary Tissue and Cells Using Taxol-Dependent Purification Combined with Microtubule-Associated Protein Specific Antibodies. *Biochemistry*, *24*(15). https://doi.org/10.1021/bi00336a055

Bloom, G. S., Luca, F. C., & Valleet, R. B. (1985). Microtubule-associated protein 1B: Identification of a major component of the neuronal cytoskeleton (monoclonal antibodies/immunofluorescence microscopy/peptide mapping/rapid axonal transport). In *Cell Biology* (Vol. 82).

Bodaleo, F. J., Montenegro-Venegas, C., Henríquez, D. R., Court, F. A., & Gonzalez-Billault, C. (2016). Microtubule-associated protein 1B (MAP1B)-deficient neurons show structural presynaptic deficiencies in vitro and altered presynaptic physiology. *Scientific Reports*, *6*. https://doi.org/10.1038/srep30069

Bouquet, C., Soares, S., Von Boxberg, Y., Ravaille-Veron, M., Propst, F., & Nothias, F. (2004). Microtubule-associate protein 1B controls directionality of growth cone migration and axonal branching in regeneration of adult dorsal root ganglia neurons. *Journal of Neuroscience*, *24*(32). https://doi.org/10.1523/JNEUROSCI.2254-04.2004

Cheng, L., Desai, J., Miranda, C. J., Duncan, J. S., Qiu, W., Nugent, A. A., Kolpak, A. L., Wu, C. C., Drokhlyansky, E., Delisle, M. M., Chan, W. M., Wei, Y., Propst, F., Samara, L. R. P., Fritzsch, B., & Engle, E. C. (2014). Human CFEOM1 mutations attenuate KIF21A autoinhibition and cause oculomotor axon stalling. *Neuron*, *82*(2), 334–349. https://doi.org/10.1016/j.neuron.2014.02.038

Chevalier-Larsen, E., & Holzbaur, E. L. F. (2006). Axonal transport and neurodegenerative disease. In *Biochimica et Biophysica Acta - Molecular Basis of Disease* (Vol. 1762, Issues 11–12). https://doi.org/10.1016/j.bbadis.2006.04.002

Chiba, K., Takahashi, H., Chen, M., Obinata, H., Arai, S., Hashimoto, K., Oda, T., McKenney, R. J., & Niwa, S. (2019). Disease-associated mutations hyperactivate KIF1A motility and anterograde axonal transport of synaptic vesicle precursors. *Proceedings of the National Academy of Sciences of the United States of America*, *116*(37), 18429–18434. https://doi.org/10.1073/pnas.1905690116

Coles, C. H., & Bradke, F. (2015). Coordinating Neuronal Actin–Microtubule Dynamics. *Current Biology*, *25*(15), R677–R691. https://doi.org/10.1016/J.CUB.2015.06.020

Dehmelt, L., & Halpain, S. (2004). Actin and Microtubules in Neurite Initiation: Are MAPs the Missing Link? In *Journal of Neurobiology* (Vol. 58, Issue 1, pp. 18–33). https://doi.org/10.1002/neu.10284

Del Río, J. A., Gonzá lez-Billault, C., Ureñ, J. M., Jimé nez, E. M., Barallobre, M. J., Pascual, M., Pujadas, L., Simó, S., & La Torre, A. (2004). MAP1B Is Required for Netrin 1 Signaling in Neuronal Migration and Axonal Guidance. *Current Biology*, *14*, 840–850. https://doi.org/10.1016/j

Dent, E. W., & Gertler, F. B. (2003). Cytoskeletal dynamics and transport in growth cone motility and guidance. In *Neuron* (Vol. 40, Issue 2). https://doi.org/10.1016/S0896-6273(03)00633-0

Evans, R. D., Robinson, C., Briggs, D. A., Tooth, D. J., Ramalho, J. S., Cantero, M., Montoliu, L., Patel, S., Sviderskaya, E. V., & Hume, A. N. (2014). Myosin-Va and dynamic actin oppose microtubules to drive long-range organelle transport. *Current Biology*, *24*(15). https://doi.org/10.1016/j.cub.2014.06.019

Garner, C. C., Garner, A., Huber, G., Kozak, C., & Matus, A. (1990). Molecular Cloning of Microtubule-Associated Protein 1 (MAP1A) and Microtubule-Associated Protein 5 (MAP1B): Identification of Distinct Genes and Their Differential Expression in Developing Brain. *Journal of Neurochemistry*, *55*(1). https://doi.org/10.1111/j.1471-4159.1990.tb08832.x

Gomi, F., & Uchida, Y. (2012). MAP1B 1-126 interacts with tubulin isoforms and induces neurite outgrowth and neuronal death of cultured cortical neurons. *Brain Research*, *1433*, 1–8. https://doi.org/10.1016/j.brainres.2011.11.028

Halpain, S., & Dehmelt, L. (2006). The MAP1 family of microtubule-associated proteins. In *Genome Biology* (Vol. 7, Issue 6). https://doi.org/10.1186/gb-2006-7-6-224

Hammarback, J. A., Obar, R. A., Hughes, S. M., & Vallee, R. B. (1991). MAP1B is encoded as a polyprotein that is processed to form a complex N-terminal microtubule-binding domain. *Neuron*, *7*(1), 129–139. https://doi.org/10.1016/0896-6273(91)90081-A

Heinzen, E. L., O'Neill, A. C., Zhu, X., Allen, A. S., Bahlo, M., Chelly, J., Chen, M. H., Dobyns, W. B., Freytag, S., Guerrini, R., Leventer, R. J., Poduri, A., Robertson, S. P., Walsh, C. A., & Zhang, M. (2018). De novo and inherited private variants in MAP1B in periventricular nodular heterotopia. *PLoS Genetics*, *14*(5). https://doi.org/10.1371/journal.pgen.1007281

Ittner, A., Chua, S. W., Bertz, J., Volkerling, A., Van Der Hoven, J., Gladbach, A., Przybyla, M., Bi, M., Van Hummel, A., Stevens, C. H., Ippati, S., Suh, L. S., Macmillan, A., Sutherland, G., Kril, J. J., Silva, A. P. G., Mackay, J., Poljak, A., Delerue, F., … Ittner, L. M. (2016). Site-specific phosphorylation of tau inhibits amyloid-β toxicity in Alzheimer's mice. *Science*, *354*(6314). https://doi.org/10.1126/science.aah6205

Jordan, M. A., & Wilson, L. (2004). Microtubules as a target for anticancer drugs. In *Nature Reviews Cancer* (Vol. 4, Issue 4, pp. 253–265). Nature Publishing Group. https://doi.org/10.1038/nrc1317

Kapitein, L. C., & Hoogenraad, C. C. (2015). Building the Neuronal Microtubule Cytoskeleton. In *Neuron* (Vol. 87, Issue 3). https://doi.org/10.1016/j.neuron.2015.05.046

Kimura, T., Hosokawa, T., Taoka, M., Tsutsumi, K., Ando, K., Ishiguro, K., Hosokawa, M., Hasegawa, M., & Hisanaga, S. I. (2016). Quantitative and combinatory determination of in situ phosphorylation of tau and its FTDP-17 mutants. *Scientific Reports*, *6*. https://doi.org/10.1038/srep33479

Kollman, J. M., Merdes, A., Mourey, L., & Agard, D. A. (2011). Microtubule nucleation by γ-tubulin complexes. In *Nature Reviews Molecular Cell Biology* (Vol. 12, Issue 11). https://doi.org/10.1038/nrm3209

Kuznetsov, S. A., Rodionov, V. I., Gelfand, V. I., & Rosenblat, V. A. (1981). Microtubule-associated protein MAP1 promotes microtubule assembly in vitro. *FEBS Letters*, *135*(2). https://doi.org/10.1016/0014-5793(81)80791-0

Lipka, J., Kapitein, L. C., Jaworski, J., & Hoogenraad, C. C. (2016). Microtubule-binding protein doublecortin-like kinase 1 (DCLK1) guides kinesin-3-mediated cargo transport to dendrites. *The EMBO Journal*, *35*(3). https://doi.org/10.15252/embj.201592929

Liu, F., Liang, Z., Wegiel, J., Hwang, Y., Iqbal, K., Grundke-Iqbal, I., Ramakrishna, N., & Gong, C. (2008). Overexpression of Dyrk1A contributes to neurofibrillary degeneration in Down syndrome. *The FASEB Journal*, *22*(9). https://doi.org/10.1096/fj.07-104539

McKenney, R. J., Huynh, W., Tanenbaum, M. E., Bhabha, G., & Vale, R. D. (2014). Activation of cytoplasmic dynein motility by dynactin-cargo adapter complexes. *Science*, *345*(6194). https://doi.org/10.1126/science.1254198

Mitchison, T., & Kirschner, M. (1984). Dynamic instability of microtubule growth. *Nature*, *312*(5991), 237–242. https://doi.org/10.1038/312237a0

Mohan, R., & John, A. (2015). Microtubule-associated proteins as direct crosslinkers of actin filaments and microtubules. In *IUBMB Life* (Vol. 67, Issue 6, pp. 395–403). Blackwell Publishing Ltd. https://doi.org/10.1002/iub.1384

Monroy, B. Y., Sawyer, D. L., Ackermann, B. E., Borden, M. M., Tan, T. C., & Ori-Mckenney, K. M. (2018). Competition between microtubule-associated proteins directs motor transport. *Nature Communications*, *9*(1). https://doi.org/10.1038/s41467-018-03909-2

Monroy, B. Y., Tan, T. C., Oclaman, J. M., Han, J. S., Simó, S., Niwa, S., Nowakowski, D. W., McKenney, R. J., & Ori-McKenney, K. M. (2020). A Combinatorial MAP Code Dictates Polarized Microtubule Transport. *Developmental Cell*, *53*(1), 60-72.e4. https://doi.org/10.1016/j.devcel.2020.01.029

Noble, M., Lewis, S. A., & Cowan, N. J. (1989). The microtubule binding domain of microtubule-associated protein MAP1B contains a repeated sequence motif unrelated to that of MAP2 and Tau. *Journal of Cell Biology*, *109*(6 II), 3367–3376. https://doi.org/10.1083/jcb.109.6.3367

Pedrotti, B., & Islam, K. (1996). Dephosphorylated but not phosphorylated microtubule associated protein MAP1B binds to microfilaments. In *FEBS 17131 FEBS Letters* (Vol. 388).

Qiang, L., Yu, W., Andreadis, A., Luo, M., & Baas, P. W. (2006). Tau protects microtubules in the axon from severing by katanin. *Journal of Neuroscience*, *26*(12). https://doi.org/10.1523/JNEUROSCI.5392-05.2006

Ramkumar, A., Jong, B. Y., & Ori-Mckenney, K. M. (2018). *ReMAPping the Microtubule Landscape: How Phosphorylation Dictates the Activities of Microtubule-Associated Proteins*. https://doi.org/10.1002/dvdy

Riederer, B. M. (2007). Microtubule-associated protein 1B, a growth-associated and phosphorylated scaffold protein. In *Brain Research Bulletin* (Vol. 71, Issue 6, pp. 541–558). https://doi.org/10.1016/j.brainresbull.2006.11.012

Roll-Mecak, A., & McNally, F. J. (2010). Microtubule-severing enzymes. In *Current Opinion in Cell Biology* (Vol. 22, Issue 1, pp. 96–103). https://doi.org/10.1016/j.ceb.2009.11.001

Roll-Mecak, A., & Vale, R. D. (2008). Structural basis of microtubule severing by the hereditary spastic paraplegia protein spastin. *Nature*, *451*(7176). https://doi.org/10.1038/nature06482

Ryoo, S.-R., Jeong, H. K., Radnaabazar, C., Yoo, J.-J., Cho, H.-J., Lee, H.-W., Kim, I.-S., Cheon, Y.-H., Ahn, Y. S., Chung, S.-H., & Song, W.-J. (2007). DYRK1A-mediated Hyperphosphorylation of Tau. *Journal of Biological Chemistry*, *282*(48). https://doi.org/10.1074/jbc.m707358200

Scales, T. M. E., Lin, S., Kraus, M., Goold, R. G., & Gordon-Weeks, P. R. (2009). Nonprimed and DYRK1A-primed GSK3β-phosphorylation sites on MAP1B regulate microtubule dynamics in growing axons. *Journal of Cell Science*, *122*(14). https://doi.org/10.1242/jcs.040162

Schneider, A., Biernat, J., Von Bergen, M., Mandelkow, E., & Mandelkow, E. M. (1999). Phosphorylation that detaches tau protein from microtubules (Ser262, Ser214) also protects it against aggregation into Alzheimer paired helical filaments. *Biochemistry*, *38*(12). https://doi.org/10.1021/bi981874p

Song, Y., Ori-McKenney, K. M., Zheng, Y., Han, C., Jan, L. Y., & Jan, Y. N. (2012). Regeneration of Drosophila sensory neuron axons and dendrites is regulated by the Akt pathway involving Pten and microRNA bantam. *Genes and Development*, *26*(14). https://doi.org/10.1101/gad.193243.112

Takei, Y., Kondo, S., Harada, A., Inomata, S., Noda, T., & Hirokawa, N. (2000). Defects in Axonal Elongation and Neuronal Migration in Mice with Disrupted tau and map1b Genes. In *The Journal of Cell Biology* (Vol. 150, Issue 5). http://www.jcb.org

Tan, R., Lam, A. J., Tan, T., Han, J., Nowakowski, D. W., Vershinin, M., Simó, S., Ori-McKenney, K. M., & McKenney, R. J. (2019). Microtubules gate tau condensation to spatially regulate microtubule functions. In *Nature Cell Biology* (Vol. 21, Issue 9, pp. 1078–1085). Nature Publishing Group. https://doi.org/10.1038/s41556-019-0375-5

Tögel, M., Wiche, G., & Propst, F. (1998). Novel Features of the Light Chain of Microtubule-associated Protein MAP1B: Microtubule Stabilization, Self Interaction, Actin Filament Binding, and Regulation by the Heavy Chain. In *The Journal of Cell Biology* (Vol. 143, Issue 3). http://www.jcb.org

Tortosa, E., Montenegro-Venegas, C., Benoist, M., Härtel, S., González-Billault, C., Esteban, J. A., & Avila, J. (2011). Microtubule-associated protein 1B (MAP1B) is required for dendritic spine development and synaptic maturation. *Journal of Biological Chemistry*, *286*(47), 40638–40648. https://doi.org/10.1074/jbc.M111.271320

Tucker, R. P. (1990). The roles of microtubule-associated proteins in brain morphogenesis: a review. In *Brain Research Reviews* (Vol. 15, Issue 2, pp. 101–120). https://doi.org/10.1016/0165-0173(90)90013-E

Tucker, R. P., Binder, L. I., & Matus, A. I. (1988). Neuronal microtubule-associated proteins in the embryonic avian spinal cord. *Journal of Comparative Neurology*, *271*(1). https://doi.org/10.1002/cne.902710106

van der Vaart, B., van Riel, W. E., Doodhi, H., Kevenaar, J. T., Katrukha, E. A., Gumy, L., Bouchet, B. P., Grigoriev, I., Spangler, S. A., Yu, K. Lou, Wulf, P. S., Wu, J., Lansbergen, G., van Battum, E. Y., Pasterkamp, R. J., Mimori-Kiyosue, Y., Demmers, J., Olieric, N., Maly, I. V., … Akhmanova, A. (2013). CFEOM1-associated kinesin KIF21A is a cortical microtubule growth inhibitor. *Developmental Cell*, *27*(2), 145–160. https://doi.org/10.1016/j.devcel.2013.09.010

Verhey, K. J., & Hammond, J. W. (2009). Traffic control: Regulation of kinesin motors. In *Nature Reviews Molecular Cell Biology* (Vol. 10, Issue 11). https://doi.org/10.1038/nrm2782

Villarroel-Campos, D., & Gonzalez-Billault, C. (2014). The MAP1B case: An old MAP that is new again. *Developmental Neurobiology*, *74*(10), 953–971. https://doi.org/10.1002/dneu.22178

Wang, Y., & Mandelkow, E. (2016). Tau in physiology and pathology. In *Nature Reviews Neuroscience* (Vol. 17, Issue 1). https://doi.org/10.1038/nrn.2015.1

Yu, H.-J., & Koh, S.-H. (2017). The role of PI3K/AKT pathway and its therapeutic possibility in Alzheimer's disease. *Hanyang Medical Reviews*, *37*(1). https://doi.org/10.7599/hmr.2017.37.1.18

Zhu, Y., Xu, J., & Heinemann, S. F. (2009). Synaptic vesicle exocytosis-endocytosis at central synapses. In *Communicative and Integrative Biology* (Vol. 2, Issue 5). https://doi.org/10.4161/cib.2.5.8896